

The geochemistry of leucite-bearing lavas from early stages of the Somma-Vesuvius volcanic complex: Feeder systems and mantle enrichment processes in the Neapolitan district of the Roman Magmatic Province

Vincenza Guarino ^{a,*}, Roberto Solone ^{a,1}, Martina Casalini ^{b,c}, Luigi Franciosi ^a, Luigi Dallai ^d, Vincenzo Morra ^a, Sandro Conticelli ^{a,b,c}, Leone Melluso ^a

^a Dipartimento di Scienze della Terra, dell'Ambiente e delle Risorse, Università degli Studi di Napoli Federico II, via Cintia, 21, 80126 Napoli, Italy

^b Dipartimento di Scienze della Terra, Università degli Studi di Firenze, via Giorgio La Pira, 4, 50121 Firenze, Italy

^c CNR - Istituto di Geologia Ambientale e Geoingegneria, Area della Ricerca Roma-1, Strada Provinciale 35d, 9, Montelibretti, 00010 Roma, Italy

^d Dipartimento di Scienze della Terra, Sapienza Università di Roma, P.le Aldo Moro, 5, 00185 Roma, Italy



ARTICLE INFO

Handling Editor: Astrid Holzheid

Keywords:

Leucite tephrites
Leucite-bearing shoshonites
Leucite-free shoshonites
Ultrapotassic volcanism
Somma-Vesuvius
Neapolitan district
Roman Province

ABSTRACT

The lavas of the Mt. Somma volcanic epoch were erupted during the early stage of the Somma-Vesuvius volcanic complex. These lavas are mildly differentiated with the presence of plagioclase-clinopyroxene-olivine- ± leucite-bearing rocks (*leucite tephrites*, *leucite-bearing shoshonites*, *latites*), also characterized by low in MgO, Cr and Ni, with a Sr-Nd-isotope range ($^{87}\text{Sr}/^{86}\text{Sr} = 0.706865\text{--}0.707861$; $^{143}\text{Nd}/^{144}\text{Nd} = 0.51244\text{--}0.51258$) that overlaps with lavas of the late stage Vesuvius erupted after 1631 CE (late stage of the Somma-Vesuvius volcanic complex). Differentiation is dominated by closed-system processes, with fractional crystallization of clinopyroxene, calcic plagioclase, olivine, magnetite, and leucite. Open-system differentiation processes are subordinate and associated with limited interaction with crustal rocks. Oxygen isotopes on clinopyroxene and olivine phenocrysts ($\delta^{18}\text{O} = 6.5\text{--}7.9\text{ ‰}$) are higher than typical uncontaminated mantle magmas, suggesting a crustal contribution to the melt. Although open-system assimilation + fractional crystallization certainly took place, this process alone does not adequately reproduce the chemical and isotopic composition of the Mt. Somma ultrapotassic magmas. Therefore, a contribution from a recycled crustal component in the mantle source is required, but probably dominated by sediment-derived fluids and melts. The Mt. Somma lavas are characterized by distinctly different geochemical features compared to the mafic products of the neighboring volcanic areas (i.e., Phlegrean, Procida and Ischia volcanic fields), where the recycled crustal component is less pronounced.

1. Introduction

The Somma-Vesuvius volcanic complex is one of the best-known volcanoes in the world, due to its location in a densely populated area, to its history related to the effects of several Plinian and sub-Plinian eruptions (e.g., 3800 yr. B.C. “Avellino”, 79 CE “Pompeii” and 472 CE “Pollena” eruptions), one of which caused the disappearance of the cities of Pompeii, Herculaneum and Stabiae. This volcano belongs to the Neapolitan district (Fig. 1), which is the southernmost volcanic cluster of the Roman Magmatic Province (e.g., Washington, 1906; Avanzinelli et al., 2009; Conticelli et al., 2004, 2010, 2015a).

The Roman Magmatic Province (RMP) occupies the Tyrrhenian side of the Apennine chain, from southern Tuscany to Naples, and is composed of several volcanic complexes of mainly Pleistocene to Quaternary age that share potassic to ultrapotassic affinities (e.g., Washington, 1906; Beccaluva et al., 1991; Conticelli et al., 2004, 2010; Avanzinelli et al., 2009, 2017; Peccerillo, 2017). Beccaluva et al. (1991) first identified a distinct geochemical and isotopic discontinuity between the Roccamonfina volcano, the southernmost parts of the Latian districts of the RMP, and the southernmost sector of the RMP belonging to the Neapolitan district (Fig. 1). This geochemical discontinuity was interpreted as the result of a different recycled sedimentary contribution

* Corresponding author at: Dipartimento di Scienze della Terra, dell'Ambiente e delle Risorse, Università degli Studi di Napoli Federico II, via Cintia, 21, 80126 Napoli, Italy.

E-mail address: vincenza.guarino@unina.it (V. Guarino).

¹ Present address: Poste Italiane.

in a slightly enriched mantle, generally thought to be similar to the source of E-MORB (e.g., D'Antonio and Di Girolamo, 1994; D'Antonio et al., 1996, 1999; Iovine et al., 2018) and/or by the occurrence of contributions from geochemical reservoirs derived from the Aeolian subduction and from a slab tear located in the Mt. Vulture area (e.g., Peccerillo, 2001, 2017; Gasperini et al., 2002; Avanzinelli et al., 2009, 2018; Conticelli et al., 2009a, 2009b, 2010, 2015a). Geochemical and radiogenic isotope data indicate that the most mafic magmas of the RMP, independently of their degree of silica saturation, were chemically influenced by subducted pelitic ± carbonate lithologies in the genesis of their variably enriched mantle sources (e.g., Conticelli et al., 2002, 2007, 2013, 2015a; Avanzinelli et al., 2008, 2009, 2018; Casalini et al., 2019). Recent studies have shown that recycling of sedimentary to crustal materials in subduction zones significantly modifies the Sr-Nd-Pb-O isotopes of metasomatized peridotite (e.g., Conticelli and Peccerillo, 1992; Iovine et al., 2018; Dallai et al., 2019, 2022; Avanzinelli et al., 2020; Fan et al., 2021).

The Somma-Vesuvius volcanic complex is a nested volcano with an early, pre-caldera, epoch that brought to the building of the Monte Somma stratovolcano, an intermediate epoch that brought to the caldera formation through several explosive Plinian to sub-Plinian eruptions, and a post-caldera epoch that built up the post-caldera Vesuvius great cone (e.g., Santacroce, 1987; Cioni et al., 1999, 2008, 2019; Avanzinelli et al., 2017). The Somma-Vesuvius volcanic complex is also well known for the occurrence of limestone and skarn xenoliths that well document the interaction between mantle-derived magmas and Mesozoic limestones and dolostones of the crustal basement of the volcano (e.g., Fulignati et al., 2005; Jolis et al., 2015; Balassone et al., 2013, 2023).

The role of the magma interaction with Mesozoic basement limestones in the genesis of the Somma-Vesuvius volcanic rocks has been historically debated (e.g., Savelli, 1967, 1968 and references therein; Di Renzo et al., 2007; Iacono Marziano et al., 2008; Conticelli et al., 2010; Dallai et al., 2011; Pichavant et al., 2014; Jolis et al., 2015; Avanzinelli et al., 2018), and more recently also for other potassic/ultrapotassic districts of the RMP (e.g., Dallai et al., 2004; Gaeta et al., 2006, 2009; Iacono Marziano et al., 2007, 2008; Freda et al., 2008; Boari et al., 2009a, 2009b). The interaction at shallow level between potassic magmas and carbonate sedimentary sequences was thought to be the main source of CO₂-bearing gases around Vesuvius. However, an important contribution of mantle-derived CO₂ to the production of Vesuvius gases has also been suggested and documented (e.g., Avanzinelli et al., 2018).

With respect to the entire sequence of the Somma-Vesuvius volcanic complex, the lavas and dikes of Mt. Somma have received little geochemical and petrological attention in the scientific literature, although they constitute the largest portion of the early stratovolcano. Indeed, previous studies of the stratovolcano focused mainly on the explosive and effusive activity of the syn- and post-caldera Somma-Vesuvius volcanic complex (e.g., Cioni et al., 1999; Melluso et al., 2022 and references therein). As a corollary, the study of the complete evolution of the Somma-Vesuvius volcanic complex may provide a case study to investigate in detail the involvement of CO₂ in the early (pre-19-21 ka) activity of the Somma-Vesuvius volcanic complex.

In this paper we report new and original geochemical and Sr-Nd-O isotope data of lavas and dikes collected along the entire stratigraphic log of Mt. Somma, sampling the caldera wall and the outer slopes in detail (Supplementary Fig. 1) to fill this gap of knowledge. The data are

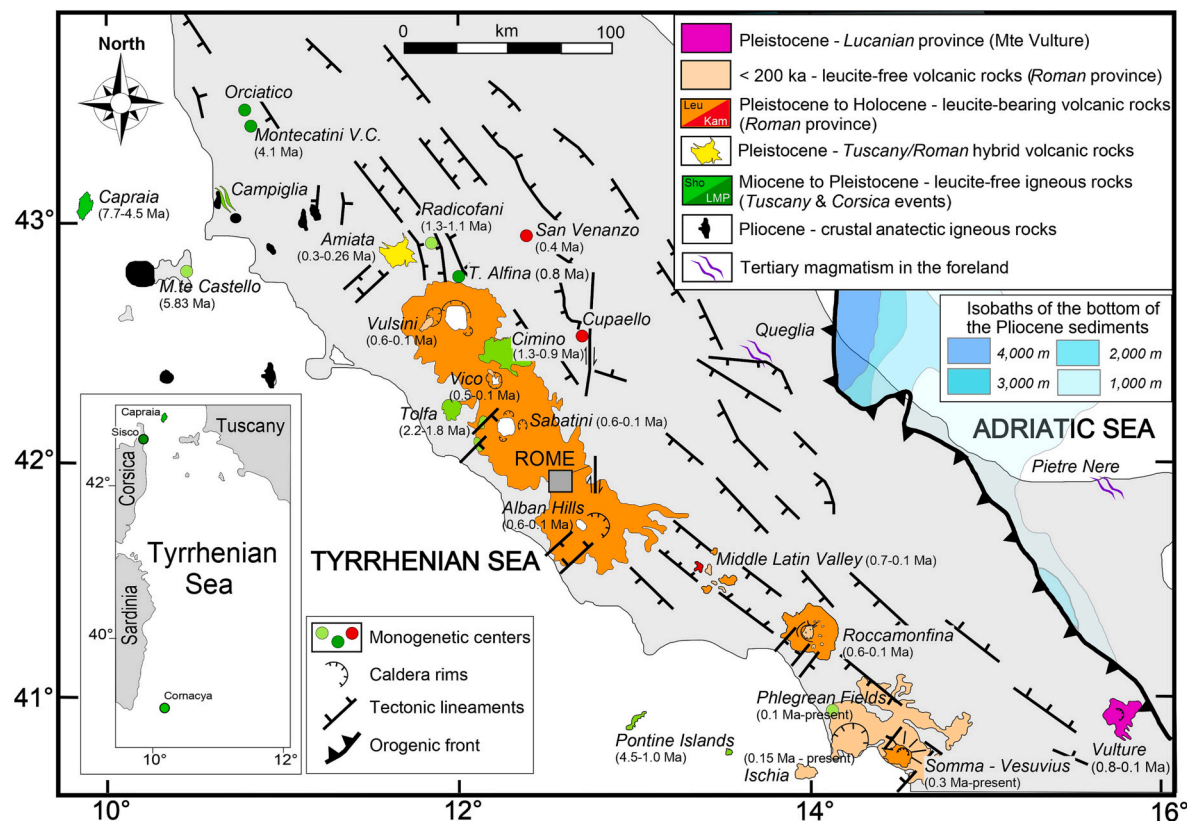


Fig. 1. Distribution of potassic and ultrapotassic volcanism associated with calc-alkaline and shoshonitic rocks in Central Italy (redrawn after Conticelli et al., 2013, 2015a, 2015b; Günther et al., 2023). Ranges of emplacement absolute ages are also reported beside each either volcanic centre or igneous rocks. For age references see: Conticelli et al., 2010, 2011, 2015a, 2015b; Laurenzi et al., 2015; Avanzinelli et al., 2017; Peccerillo, 2017. Roma Magmatic Province is reported on the bases of silica saturations and leucite occurrence (i.e., Red, Orange, and light Brown). Latian districts are those from Vulcini, at North, and Roccamontefina, at South. Neapolitan district is the southernmost volcanic cluster made of Ischia, Procida, Phleorean Fields, and Somma-Vesuvius volcanoes (after Avanzinelli et al., 2009). The Monte Amiata volcano is a hybrid potassic volcano with magmas generated by mixing between the Tuscany and Roman magmatic provinces (van Bergen et al., 1983; Conticelli et al., 2015b). (For interpretation of the references to color in this figure legend, the reader is referred to the web version of this article.)

discussed in the broader context of the petrological evolution of the Somma-Vesuvius volcanic rocks to better elucidate the processes that led to the transition from slightly to highly silica undersaturated magmas through time. The geochemical characteristics thought to be mantle-related, and the importance of the Mt. Somma magmas in the RMP are also highlighted.

2. Geological setting

The Somma-Vesuvius volcanic complex is located in the Neapolitan district (Fig. 1), together with the Phleorean Fields, Procida and Ischia volcanoes (e.g., Washington, 1906; Beccaluva et al., 1991; Avanzinelli et al., 2009; Conticelli et al., 2010, 2015a, 2015b), south of the Roccamonfina volcano and overlying the 2 Ma buried calc-alkaline andesites found in the Parete and Castel Volturno boreholes (e.g., Beccaluva et al., 1991; Di Girolamo et al., 1996; Rouchon et al., 2008; Conticelli et al., 2010; Avanzinelli et al., 2017).

The Somma-Vesuvius volcanic complex consists of an ancient stratovolcano, the Mt. Somma stratocone, with a summit caldera in which the younger Vesuvius Great Cone (s.s.) is nested. The pre-caldera summit of the Mt. Somma volcano was probably located about 500 m north of the present-day crater, at an elevation of about 1600–1900 m.a.s.l. Samples from the “Trecase 1” geothermal well have been dated to 320–360 ka, but it is highly uncertain whether these samples belong to the Somma-Vesuvius activity (cf. Brocchini et al., 2001). The activity of Mt. Somma is earlier than the Plinian “Pomici di Base” eruption. Most of the products of the ancient Somma volcano are exposed in the inner walls of the caldera, with pyroclastic deposits found in the Camaldoli della Torre borehole (SE of the Vesuvius cone) interlayered with the products of the Campanian Ignimbrite eruption (Di Renzo et al., 2007). Three large explosive events occurred between 39 and 22 ka: the “La Schiava” eruption (36 ka), the “Taurano” eruption (36–33 ka), the “Codola” eruption (33 ka), and the “Carcavone” eruption (39–22 ka) (Sparice et al., 2017 and references therein). Other Plinian eruptions are known: the “Pomici di Base” eruption (21,670 yr BP), the “Pomici Verdone” eruption ($16,130 \pm 110$ yr. BP), the “Mercato” eruption (a.k.a. “Ottaviano” eruption, 8900 yr. BP); the “Avellino” eruption (3945 ± 10 cal BP), the “Pompeii” eruption (79 CE) and the “Pollena” eruption (472 CE) (e.g., Melluso et al., 2022 and references therein). After minor activity just after the 472 CE and medieval activity, the last period of activity started in 1631 CE with a mild and semi-persistent activity, with minor lava effusions and short quiescent periods (last event 1944 CE). Each quiescent period was preceded by relatively powerful explosive effusive polyphase eruptions.

Tomographic images of the volcano reveal a central cylindric core of high rigidity below the axial area of the volcano (e.g., Zollo et al., 1996; Fedi et al., 2018 and references therein), which has been interpreted as a solidified magmatic intrusion or conduit. A sharp decrease in P-wave velocity is observed below 9–10 km depth; this feature is thought to be evidence for a magma reservoir (e.g., Zollo et al., 1996; Piana Agostinetti and Chiarabba, 2008).

3. Materials, methods, and classification of Mt. Somma volcanic rocks

Fresh samples of lavas (n. samples: 95) and dikes (n. samples: 5), representative of the pre-caldera volcanic history, were collected along the slopes of Mt. Somma (Fig. 2; Supplementary Fig. 1). Analytical techniques are described in detail in the Supplementary Material 1 (see Cucciniello et al., 2017, 2022; Guarino et al., 2021). Majors and trace elements, determined by ICP-OES and ICP-MS, are reported in Table 1, while XRF analyses are reported in Supplementary Table 1. Detailed petrographic description, mineral chemistry, and crystallization conditions are given in Supplementary Material 2. Analyses of radiogenic isotopes were carried out on rock powders of selected samples preliminarily treated with 2.5 M HCl for 4 h and then rinsed three times with

Milli-Q water, as leaching generally minimize isotopic variation – induced by supergene processes – that may overprint the magmatic signature. Sr–Nd isotopic ratios were determined after purification using thermal ionization mass spectrometry (Thermo-Fisher Scientific Triton™) at the Dipartimento di Scienze della Terra of the University of Florence, with the methods described by (Avanzinelli et al., 2005, 2020, and references therein) and then reported in Table 1.

The Mt. Somma lavas and dykes were classified according to the K₂O-Na₂O diagram of Middlemost (1975), Total Alkali vs. Silica (T.A.S., Le Bas et al., 1986), the K₂O-SiO₂ diagram (Di Girolamo, 1984), the R1-R2 classification diagram (de la Roche et al., 1980) to the criteria of Foley et al. (1987) (Fig. 3a-d) and CIPW norms (Supplementary Table 1). Overall, the Mt. Somma lavas and dikes are *nepheline*-normative and subordinately *leucite*-normative (Supplementary Table 1); the potassic volcanic rocks are the least silica-undersaturated. Leucite-bearing lavas are divided into three main groups according to the degree of silica saturation:

(1) *Leucite tephrites* (s.l.): This group is formed by leucite-bearing lavas with leucite both as phenocrysts and in the CIPW norm. These rocks are highly silica undersaturated (SSU) [*leucite*-normative, *leucite* (lc) = 8–22 %; *nepheline* (ne) = 11–17 %] with terms ranging from leucite-tephrite to leucite-tephriphonolite (Fig. 3c, d). This group is strictly equivalent in terms of mineralogy, petrography (Supplementary Material 2.1) and chemical composition to the lavas of the recent Vesuvius Great Cone activity (1631–1944 CE).

(2) *Leucite-bearing shoshonites*: This group of rocks consists of leucite-bearing rocks without leucite in the CIPW norm. These rocks plot in the latite and shoshonite fields of the TAS and R1-R2, with a few samples crossing the boundary with tephrites (Fig. 3c, d; Supplementary Material 2.1). Since the normative *nepheline* is variable but significantly high (2–13 %), these rocks are slightly to moderately silica undersaturated (hereafter MSU).

(3) *Leucite-free shoshonites*: This lava group has K₂O/Na₂O < 2 and plots in the field of potassic series in the Na₂O-K₂O diagram and in the shoshonitic field of the K₂O-SiO₂ diagram (Fig. 3a, b; Supplementary Material 2.1). In the TAS and R1-R2 diagrams, these rocks plot mainly in the latite field (hereafter *latites*) (Fig. 3c, d).

The distinction between the MSU and SSU groups corresponds to a lithologic discontinuity and a marked change in slope noted along the caldera wall, where the SSU overlie the Mt. Somma lavas and dikes (Supplementary Material 2.1).

4. Major- and trace element geochemistry

The concentration of MgO in the Mt. Somma lavas and dikes ranges from 5.8 to 2.0 wt%, with Cr and Ni < 114 and < 54 ppm, respectively; the relatively low forsterite content of olivine and the low Mg# of clinopyroxene phenocrysts (Supplementary Material 2.2) indicate that none of these rocks have compositions that can be attributed to liquids in equilibrium with a mantle source. Concentrations of CaO, Al₂O₃, Na₂O, SiO₂, Sc, and V decrease with MgO, whereas TiO₂, Fe₂O₃, P₂O₅, K₂O, and other elements have a more limited correlation (Supplementary Fig. 2). These variations seem to be compatible with the removal of an assemblage of the observed phenocryst phases. The increase in Al₂O₃ and the decrease in CaO, Sc, and V indicate a more significant removal of clinopyroxene and magnetite than of plagioclase and leucite (Supplementary Figs. 2 and 3). For a given MgO, variations in major oxides and trace elements such as Zr, Sr, Y, and Nb are not fully consistent with simple fractional crystallization schemes of the observed phases (Supplementary Fig. 3).

The bulk compositions of Mt. Somma volcanic rocks have a significant compositional range for fluorine (SSU group: F = 1079–2105 ppm; MSU group: F = 1046–2103 ppm; Latite group: F = 1061–1475 ppm) and chlorine (SSU group: Cl = 137–4551 ppm; MSU group: Cl = 46–1766 ppm; Latite group: Cl = 40–358 ppm), while S is significant in two SSU samples (69 and 1903 ppm) (Supplementary Fig. 3). Therefore,

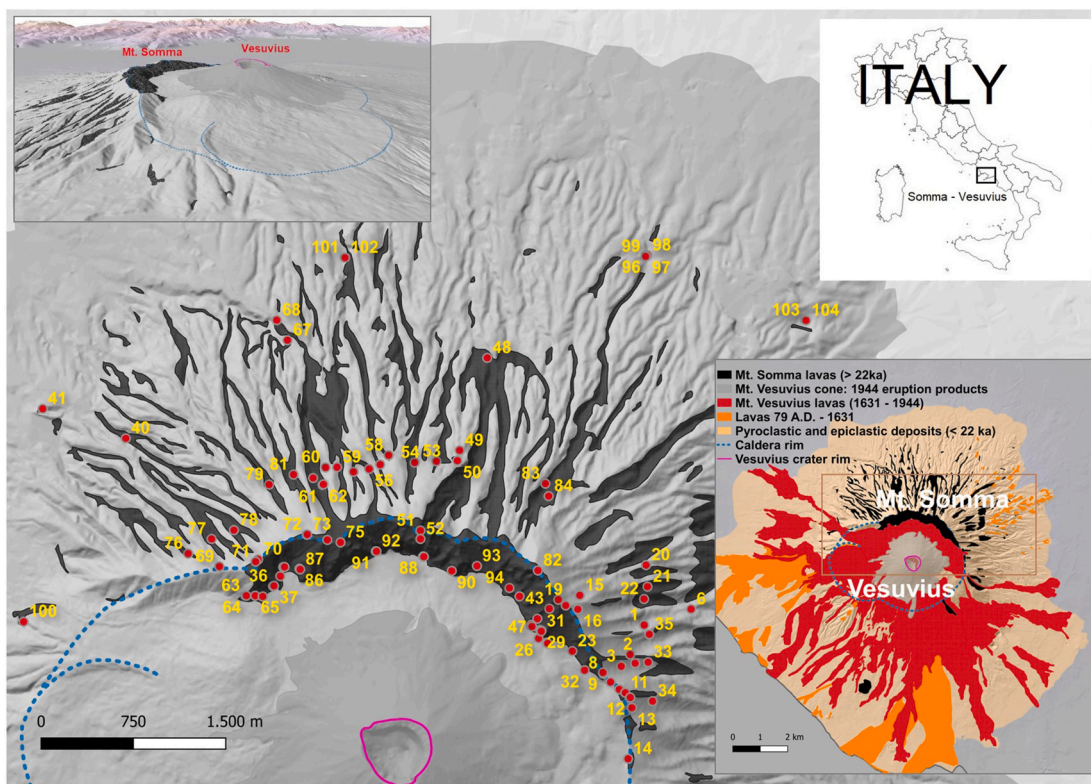


Fig. 2. Sketch map of the Somma-Vesuvius complex with red dots indicating the location of the samples studied. The dashed lines represent the boundaries of the craters of Somma (in blue), and Vesuvius (in magenta) as also reported in (a). (b) Location of Somma-Vesuvius. (c) Simplified geological map of Mt. Somma and Vesuvius, showing the outcrops of different eruptions. (For interpretation of the references to color in this figure legend, the reader is referred to the web version of this article.)

the contribution of F and Cl in the petrogenesis of the Mt. Somma lavas should be considered.

The chondrite normalized REE patterns of the Mt. Somma lavas and dikes are moderately LREE enriched ($\text{La}_{\text{N}}/\text{Yb}_{\text{N}} = 15–27$) and with significant Eu troughs [$\text{Eu}/\text{Eu}^* = \text{Eu}_{\text{N}}/(\text{Sm}_{\text{N}} \times \text{Gd}_{\text{N}})^{0.5} = 0.8–0.9$], typical of all the mafic leucite-bearing rocks of the RMP (e.g., Rogers et al., 1985; Boari et al., 2009b; Fig. 4). No significant differences are observed with increasing degree of differentiation (MgO concentration as a proxy) and group affinity, indicating that the europium (Eu) trough of the chondrite normalized patterns is not related to plagioclase removal.

The Mt. Somma lavas and dikes have Nb/Yb (11–25), Th/Yb (6–13), and Ba/Nb (37–83) ratios are significantly higher than mantle or MORB reference values (cf. Lyubetskaya and Korenaga, 2007), whereas the La/Nb ratio (1.4–2) is only slightly higher (Table 1; Fig. 5). The Zr/Hf (40–50) and Nb/Ta (16–23) ratios are also slightly higher than typical mantle ratios, Nb/U is low (4–10), and Th/U (2.7–3.7) is slightly low compared to the typical mantle ratios. The mantle-normalized multi-element patterns of the Monte Somma lavas have troughs at Nb, Ta, and Ti, a peak at Pb and marked Large Ion Lithophile Element (LILE) enrichment compared to HFSE (Fig. 6). Zr and Hf are not markedly depleted relative to the neighboring REE.

5. Nd, Sr, and O isotope composition of the Mt. Somma lavas

The Mt. Somma lavas have $^{87}\text{Sr}/^{86}\text{Sr}$ ranging from 0.706865 ± 6 to 0.707861 ± 8 and $^{143}\text{Nd}/^{144}\text{Nd}$ ranging from 0.512441 ± 5 to 0.512582 ± 6 , with no systematic variation with the degree of magmatic differentiation (Table 1; Fig. 7). These data match the known isotopic ranges of Somma-Vesuvius (e.g., 25 ka to the medieval and 1631–1944 CE eruptions; Fig. 7), but also with more differentiated rocks from the Neapolitan district (i.e., trachyte). On the other hand, the Sr–Nd isotopic ranges of Vesuvius are clearly different from the isotopic composition of

the primitive basalts of Procida (Solchiaro Mg-rich lavas) and Ischia, which represent the most primitive volcanic products erupted in the Phlegrean-Ischian volcanic areas (Fig. 7), excluding any comagmatic origin of the mafic magmas of the various volcanic districts.

The oxygen isotope composition of the Somma-Vesuvius lavas has been studied using the $\delta^{18}\text{O}$ of clinopyroxene and olivine. Clinopyroxene is ubiquitous in these rocks, and its chemical composition is sensitive to carbonate assimilation (Dallai et al., 2004). In MSU rock, clinopyroxene has $\delta^{18}\text{O}$ ranging from +6.3 to +7.9 ‰ (Table 2), and olivine has $\delta^{18}\text{O}$ between 6.4 and 7.0 ‰, thus significantly higher than clinopyroxene in an unmodified upper mantle ($\delta^{18}\text{O} = 5.6 \pm 0.3$ ‰; Matthey et al., 1994; Eiler, 2001). Considering the expected $\delta^{18}\text{O}_{\text{melt-cpx}}$ and $\delta^{18}\text{O}_{\text{melt-ol}}$ (0.2 ‰, and 0.6 ‰, respectively) (e.g., Taylor and Sheppard, 1986; Chiba et al., 1989; Matthews et al., 1998; Zhao and Zheng, 2003), equilibrium melt compositions range significantly above uncontaminated mantle-derived magmas from unmodified sources. Moreover, the negative $\delta^{18}\text{O}_{\text{cpx}}$ and Cr- $\delta^{18}\text{O}_{\text{cpx}}$ as well as Fo- $\delta^{18}\text{O}_{\text{ol}}$ covariation trends (Fig. 8a) of the MSU samples indicate that the oxygen isotope composition of the melts increased with the degree of magmatic evolution, thereby implying that crustal (carbonate) contamination occurred at least at crustal levels.

6. Discussion

The mildly silica undersaturated (MSU) and the leucite-free shoshonitic and latite rocks of Mt. Somma volcano do not represent just “a few outliers” as previously reported (e.g., Joron et al., 1987; Peccerillo, 2005; Santacroce et al., 2008), but rather, they form the bulk of the eruptive units of the first stage of the Mt. Somma-Vesuvius volcanic complex. Although the well-known transition to more silica undersaturated products is evident, it appears that it should not be considered as sharp as previously thought. In addition, some of the mildly silica

Table 1

New ICP-OES, ICP-MS analyses and Sr–Nd isotopes of the Mt. Somma lavas and dikes.

Sample	SSU group				MSU group												Latite group									
	MRL3	MRL19	MRL97V	MRL59	MRL25	MRL41	MRL43	MRL74	MRL32	MRL6	MRL27	MRL50	MRL91	MRL24	MRL48	MRL35	MRL21	MRL37	MRL103	MRL104	V44lava					
Type	Lava	Lava	Lava	Lava	Dyke	Lava	Dyke	Lava	Lava	Lava	Lava	Lava	Lava	Lava	Lava	Lava	Lava									
SiO ₂ (wt%)	49.93	48.49	51.01	50.86	51.09	49.84	51.16	51.51	51.70	51.28	51.20	52.20	53.26	51.92	51.93	53.07	51.54	53.24	53.12	53.10	48.31					
TiO ₂	1.11	0.99	1.09	1.02	0.99	1.15	0.97	0.91	0.88	0.97	0.91	0.87	1.02	0.97	0.94	0.96	0.91	1.00	1.00	1.01	1.01	0.88				
Al ₂ O ₃	16.31	16.06	16.89	16.15	16.78	16.19	17.27	17.41	17.27	17.82	17.75	17.36	17.06	17.27	17.84	17.62	17.85	17.57	17.64	17.56	18.57					
Fe ₂ O ₃ Tot	8.61	8.45	7.91	8.52	8.11	8.80	8.25	7.95	8.08	7.53	7.27	7.26	7.99	8.34	7.32	7.93	7.13	7.73	7.82	7.85	7.85	8.26				
MnO	0.15	0.15	0.14	0.14	0.14	0.15	0.14	0.14	0.13	0.13	0.12	0.12	0.13	0.14	0.12	0.13	0.12	0.13	0.13	0.13	0.13	0.15				
MgO	4.58	5.21	3.88	5.53	4.86	4.38	4.32	4.19	4.10	3.94	3.91	3.86	3.71	3.52	3.47	3.45	3.40	3.07	3.28	3.13	3.55					
CaO	9.01	10.63	7.56	9.43	9.22	9.09	8.82	8.27	8.19	8.61	8.12	7.98	7.52	7.50	8.15	7.25	8.13	7.42	7.51	7.32	8.46					
Na ₂ O	2.66	2.76	3.49	2.09	2.24	2.82	2.49	2.46	2.78	2.68	2.49	2.30	3.47	2.33	2.49	2.71	2.51	2.81	2.56	2.78	2.65					
K ₂ O	6.12	6.04	6.55	5.31	5.60	5.97	5.52	6.14	5.80	5.97	7.18	7.07	4.85	6.80	6.62	5.91	7.30	5.99	5.95	6.06	7.87					
P ₂ O ₅	1.01	0.81	0.97	0.60	0.61	1.09	0.62	0.59	0.62	0.68	0.66	0.61	0.63	0.81	0.71	0.61	0.70	0.64	0.61	0.67	0.76					
LOI	0.14	0.71	0.39	0.03	0.24	0.06	0.06	0.32	0.08	0.24	0.13	0.08	0.06	0.01	0.36	1.09	0.15	0.42	0.51	0.65	0.39					
sum	99.6	100.3	99.9	99.7	99.9	99.5	99.6	99.9	99.6	99.7	99.7	99.7	99.6	100.0	100.7	99.7	100.0	100.1	100.1	100.3	99.8					
Sc (ppm)	21	24	14	27	24	22	20	21	18	19	18	21	18	17	17	17	14	16	18	17	13					
V	212	219	250	202	254	183	201	185	155	188	191	202	238	219	195	206	177	228	148	157	212					
Cr	100	bdl	bdl	74	bdl	60	109	56	62	60	90	6	50	90	10	40	bdl	53	bdl	bdl	30					
Ni	46	32	20	37	30	30	47	36	40	30	47	16	40	50	50	30	28	35	bdl	bdl	20					
Cu	59	95	120	70	120	80	68	61	58	80	52	45	50	80	59	60	56	93	30	40	110					
Zn	69	88	80	75	70	60	69	78	78	70	83	83	80	80	88	80	88	84	90	90	80					
Rb	214	302	321	271	322	325	188	242	267	264	247	256	230	280	254	294	244	241	255	242	298					
Sr	750	993	1089	834	1006	753	806	938	849	1014	790	839	1225	957	892	1210	834	1305	958	984	1080					
Y	25	27	23	21	23	19	21	22	23	20	24	23	27	22	23	22	24	30	26	26	22					
Zr	201	215	192	180	201	170	178	195	222	191	188	219	217	207	220	217	230	309	255	260	205					
Nb	22	27	33	25	33	24	24	29	32	31	28	29	58	35	29	43	30	50	37	37	31					
Cs	12.4	17.7	19.0	13.1	15.0	19.6	10.0	12.3	13.6	14.5	9.9	12.5	12.8	14.1	12.3	15.8	12.5	13.4	13.4	13.3	17.6					
Ba	1410	2120	2187	1622	2064	1783	1985	2281	1820	2370	1400	1869	2122	2139	2006	2109	1880	2559	1577	1587	2359					
La	44.6	53.2	51.8	37.5	51.7	39.8	41.3	46.5	44.1	50.5	41.4	44.3	86.8	52.9	46.0	61.9	44.5	84.6	57.3	57.1	52.3					
Ce	93.1	108	107	77.0	106	79.8	84.1	94.2	87.8	102	83.0	89.7	171	107	93.9	118	88.2	162	113	115	106					
Pr	11.3	12.8	12.4	9.23	12.3	9.29	9.83	11.0	10.1	11.7	9.69	10.5	18.5	12.3	10.9	12.7	10.2	18.5	12.8	12.9	12.4					
Nd	46.7	50.1	47.6	36.0	46.7	34.7	37.3	42.0	39.9	42.8	38.6	40.3	66.8	46.7	40.8	45.6	39.9	67.6	47.0	48.6	48.2					
Sm	10.3	10.5	10.0	7.2	10.0	7.0	7.5	8.5	8.1	9.1	7.9	7.9	12.5	9.7	8.0	9.0	7.8	13.0	9.0	9.2	9.4					
Eu	2.53	2.65	2.30	1.80	2.34	1.71	1.88	2.17	2.02	2.16	2.07	1.93	2.98	2.19	2.01	2.08	1.98	3.09	2.20	2.30	2.45					
Gd	7.9	8.2	7.4	5.7	7.6	5.2	5.9	6.7	6.1	6.8	6.6	6.1	9.3	7.6	6.2	6.4	9.7	6.8	6.7	7.3						
Tb	1.1	1.1	1.0	0.8	1.1	0.7	0.8	0.9	0.9	0.9	0.8	1.2	1.0	0.8	0.8	0.9	1.3	0.9	1.0	0.9						
Dy	5.2	5.2	5.0	4.1	5.2	4.0	4.2	4.4	4.3	4.5	4.6	4.3	6.0	5.0	4.3	4.4	4.3	6.2	5.2	5.0						
Ho	0.9	0.9	0.9	0.7	0.9	0.7	0.7	0.7	0.8	0.8	0.8	0.8	1.0	0.9	0.7	0.8	0.8	1.0	0.9	0.9	0.9					
Er	2.3	2.5	2.4	1.9	2.5	1.9	1.9	2.0	2.0	2.2	2.2	2.1	2.7	2.3	2.0	2.3	2.1	2.6	2.6	2.6	2.4					
Tm	0.32	0.34	0.33	0.28	0.34	0.27	0.28	0.27	0.29	0.31	0.31	0.30	0.37	0.33	0.29	0.32	0.30	0.36	0.37	0.33						
Yb	2.0	2.1	2.1	1.8	2.0	1.7	1.8	1.8	1.9	1.9	2.0	2.3	2.0	1.9	1.9	1.9	2.3	2.4	2.4	2.0						
Lu	0.28	0.31	0.30	0.28	0.31	0.26	0.28	0.29	0.27	0.30	0.28	0.31	0.35	0.31	0.30	0.29	0.28	0.35	0.37	0.36	0.29					
Hf	4.9	4.6	4.5	4.1	5.0	3.7	4.0	4.3	4.6	4.3	4.2	4.9	5.1	4.6	4.8	4.3	4.8	6.6	5.6	5.7	4.3					
Ta	1.3	1.4	1.8	1.6	1.8	1.2	1.5	1.7	1.7	1.4	1.4	1.8	2.5	1.9	1.9	2.3	1.6	3.1	2.0	2.2	1.7					
Pb	bdl	36	30	23	31	30	28	34	24	29	20	30	26	30	29	40	29	33	33	31	27					
Th	15.0	18.3	20.7	14.3	18.2	14.7	13.9	17.8	16.1	18.6	12.0	17.3	20.1	17.0	17.9	24.3	16.0	24.8	19.6	19.5	18.7					
U	5.3	6.1	7.8	4.9	5.7	4.6	4.2	4.8	5.3	5.9	4.1	5.5	5.8	6.4	5.9	7.9	5.3	6.9	6.5	5.6	6.3					
⁸⁷ Sr/ ⁸⁶ Sr	0.707426	0.707861	0.707367	0.707025	0.707130	0.707513	0.707817	0.707650	0.707811	0.707120	0.707691	0.706865	0.707634	0.707771	0.707011	0.707756	0.706879									
2 s *10 ⁻⁶	±7	±8	±6	±6	±6	±7	±7	±5	±7	±7	±6	±6	±5	±7	±5	±6	±6	±6	±6	±7						
¹⁴³ Nd/ ¹⁴⁴ Nd	0.512467	0.512441	0.512486	0.512489	0.512505	0.512475	0.512454	0.512473	0.512461	0.512498	0.512455	0.512582	0.512487	0.512444	0.512504	0.512447	0.512547									
2 s *10 ⁻⁶	±4	±5	±6	±5	±6	±5	±4	±4	±5	±5	±5	±6	±4	±4	±5	±5	±4	±4	±5	±4	±5					

Note: bdl, below detection limits.

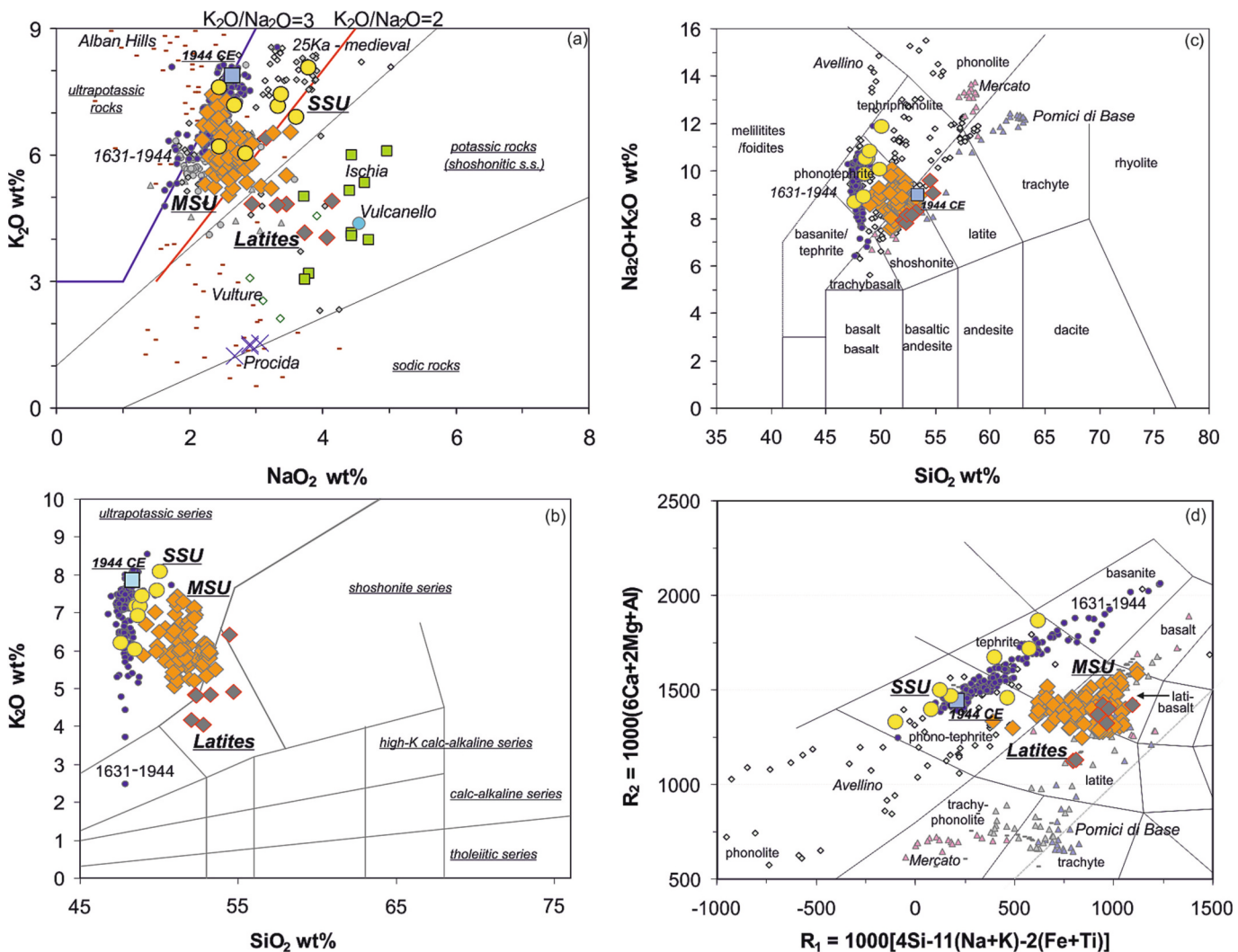


Fig. 3. (a) K_2O vs Na_2O diagram of Middlemost (1975) for the Mt. Somma samples and the lava of 1944 CE. (b) K_2O vs. SiO_2 diagram (Di Girolamo, 1984) for the Mt. Somma samples and the 1944 CE lava. The 1631–1944 volcanic products are shown. (c) TAS (Le Bas et al., 1986) and (d) R_1 - R_2 (de la Roche et al., 1980) classification diagrams for the Mt. Somma samples and 1944 CE lava. The data used for comparison are from the following references: Avanzinelli et al. (2018); Ayuso et al. (1998); Belkin et al. (1993); Boari et al. (2009a, 2009b); Cioni et al. (1998); D'Antonio et al. (1999); De Astis et al. (2006); Di Renzo et al. (2007); Fedele et al. (2008); Joron et al. (1987); Landi et al. (1999); Marianelli et al. (1999); Melluso et al. (2012, 2014, 2022); Piochi et al. (2006); Savelli (1967, 1968).

undersaturated (MSU) rocks also have a distinctly “intermediate” character, unlike the other rocks. Their occurrence is never negligible or even unrecorded. These simple observations provide interesting clues for the understanding of the petrological model for the Somma-Vesuvius volcanic complex, which justifies the presence of mafic rocks with varying degrees of silica undersaturation. The Mt. Somma lavas have their counterparts in the mafic products of the “Pomici di Base” pyroclastic eruption, which range in composition from leucite shoshonite to trachyte (e.g., Landi et al., 1999; Melluso et al., 2022), and are therefore part of a slightly silica undersaturated rock suite that is not comagmatic with the rest of the Somma-Vesuvius phonolites.

6.1. Carbon dioxide: magma differentiation vs. magma genesis

In the Somma-Vesuvius magmatic system, the CO_2 content of the magmas may reflect the effects of three main processes:

- i) fractional crystallization of the observed phenocrysts, with a limited (though significant) role of limestone assimilation (e.g., Savelli, 1968),

- ii) limestone assimilation as the main process leading to the progressive increase in alkalinity and degree of silica-undersaturation of the Somma-Vesuvius magmas (e.g., Rittmann, 1933; Iacono Marziano et al., 2007),
- iii) the dominance of deep processes with origin of the CO_2 mainly from a flux within the mantle (Avanzinelli et al., 2018).

Magma-carbonate interaction is a multistep process leading to the formation of a skarn shell, magmatic cumulates, and possibly driving melt differentiation (e.g., Savelli, 1967). Crustal contamination of magmas can occur through assimilation of solid material (carbonate and/or skarn), and carbonate-derived CO_2 flux (Dallai et al., 2011). Melt-carbonate interaction results in geochemical contamination of the melt coupled with intense CO_2 vesiculation at the melt-carbonate interface. In contrast, melt homogenization by physical mixing and mingling promoted by exsolving volatiles is a much slower process, due to the low ability of silicate and carbonate melts to mix on a syn-eruptive timescale (e.g., Deegan et al., 2010; Jolis et al., 2013; Gozzi et al., 2014).

The chemical composition of the Somma-Vesuvius magmas shifts from the moderately silica undersaturated lavas of Monte Somma to the highly silica undersaturated products of Vesuvius, a feature not

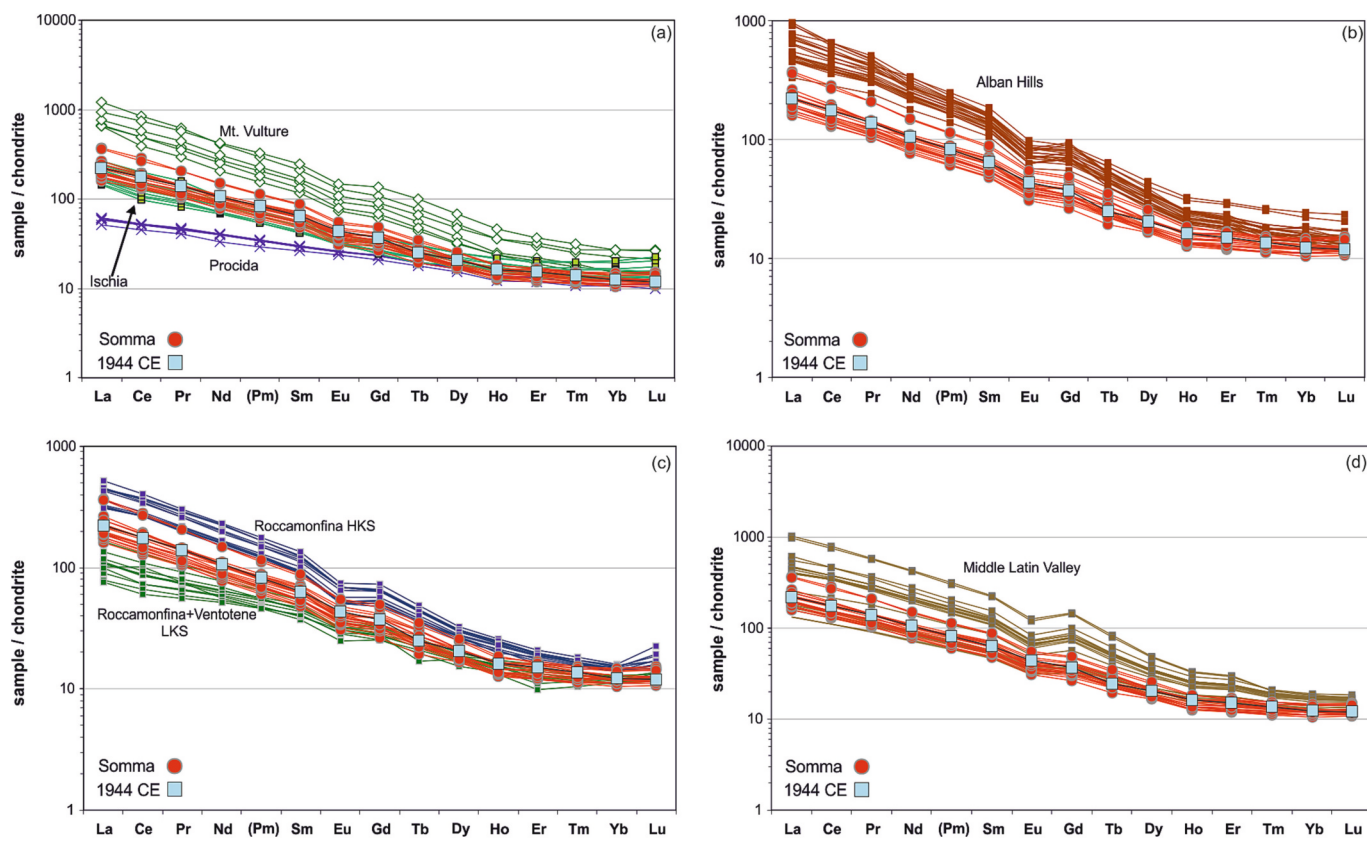


Fig. 4. Chondrite-normalized REE patterns for Mt. Somma lavas and dikes and 1944 CE lava compared with Mt. Vulture, Procida, Alban Hills, Roccamontina, Ventotene, and Middle Latin Valley rocks (Beccaluva et al., 1991, 2002; Boari et al., 2009a, 2009b; Conticelli et al., 2009b; De Astis et al., 2006). The normalization values are from Anders and Grevesse (1989). Prometium is interpolated.

observed in the nearby Phleorean Fields, Procida, Ischia and the opposite of what is found at Roccamontina and the Alban Hills (e.g., Conticelli et al., 2009b and references therein; Boari et al., 2009a, 2009b). Some authors associate the increasing degree of silica undersaturation with increasing carbonate assimilation (e.g., Freda et al., 2008; Iacono Marziano et al., 2007; Mollo et al., 2010; Jolis et al., 2015; Carter and Dasgupta, 2016). Interaction of the magma with basement limestone may have resulted in the occurrence of variably silica undersaturated rock series, starting from a single, weakly undersaturated, potassic parental magma. The model proposed by Iacono Marziano et al. (2007) suggests that the transition from the weakly undersaturated magmas of Monte Somma to the progressively more undersaturated magmas of the following periods can be achieved by carbonate assimilation (up to 15–17 %) and clinopyroxene removal (35–50 %). However, a detailed scrutiny indicates that magma-wall rock interaction cannot involve significant mass exchange (specifically CaO), due to the development of a solidification front and a Ca-phases-rich skarn shell at the boundary between the crystallizing magmas and the limestone wall rocks (e.g., Savelli, 1967; Del Moro et al., 2001). Carbonate decomposition may be responsible for a more extensive mass exchange during crust-magma interaction at the continental crustal level (e.g., Deegan et al., 2010; Mollo et al., 2010; Carter and Dasgupta, 2016). This implies that crustal contamination of magmas could occur through assimilation of solid material, although carbonate and skarn may produce opposite effects on the CO₂ increase within the magma, rather than crustally derived CaO-rich melt (Di Rocco et al., 2012) and carbonate-derived CO₂ flux (Dallai et al., 2011). As shown by Mollo et al. (2010), the presence of a CO₂-rich fluid phase during carbonate assimilation can significantly affect partition coefficients and the redox state of carbonated systems. However, crustal contamination, and in particular carbonate contamination of potassic to ultrapotassic magmas at the continental crustal level, can be

extremely difficult to be resolved from source contamination, due to the occurrence of crustal enrichment of ultrapotassic magmas from subducted crustal rocks and sediments, either carbonate-poor or carbonate-rich, which strongly modify the O-Sr-Nd-Pb isotopic composition of the mantle source (e.g., Conticelli et al., 2015a, 2015b; Avanzinelli et al., 2018, 2020; Iovine et al., 2018; Dallai et al., 2019, 2022; Chen et al., 2021, 2023; Bragagni et al., 2022). Indeed, several papers have pointed out that the assimilation of limestone or marl by a potassiac magma at the crustal level does not satisfy geochemical models to produce strongly produce silica undersaturated ultrapotassic rocks, suggesting that processes took place mainly at depth, within the mantle, but this effect was amplified by shallow level contamination within the crust (e.g., Boari et al., 2009a, 2009b; Conticelli et al., 2015a, 2015b; Ren et al., 2024).

6.2. Relationships between MSU, Latites (leucite-free rocks) and SSU (Vesuvius-like)

Quantitative models of fractional crystallization processes using major oxides were tested to model the full range of Mt. Somma epoch magmas, starting with the most “primitive” compositions (Stormer and Nicholls, 1978). The results are summarized in Supplementary Table 2.

The major oxide transition from the least to the most evolved lava compositions of the highly silica undersaturated (SSU) rocks (samples MRL3 to MRL97v; *Vesuvius-like*) was adequately modeled with a maximum 42 % removal of clinopyroxene-rich leucite-gabbro (essexite) solid (~51 wt% clinopyroxene, ~18 wt% plagioclase, ~20 wt% leucite, ~5 wt% magnetite, ~3 wt% olivine, and ~3 wt% apatite; $\Sigma R^2 = 0.180$). The tested transitions between the highly silica undersaturated rocks (sample MRL18, SSU), the latite (sample MRL71), and mildly silica undersaturated rocks (sample MRL39, MSU) were modeled with 35–47

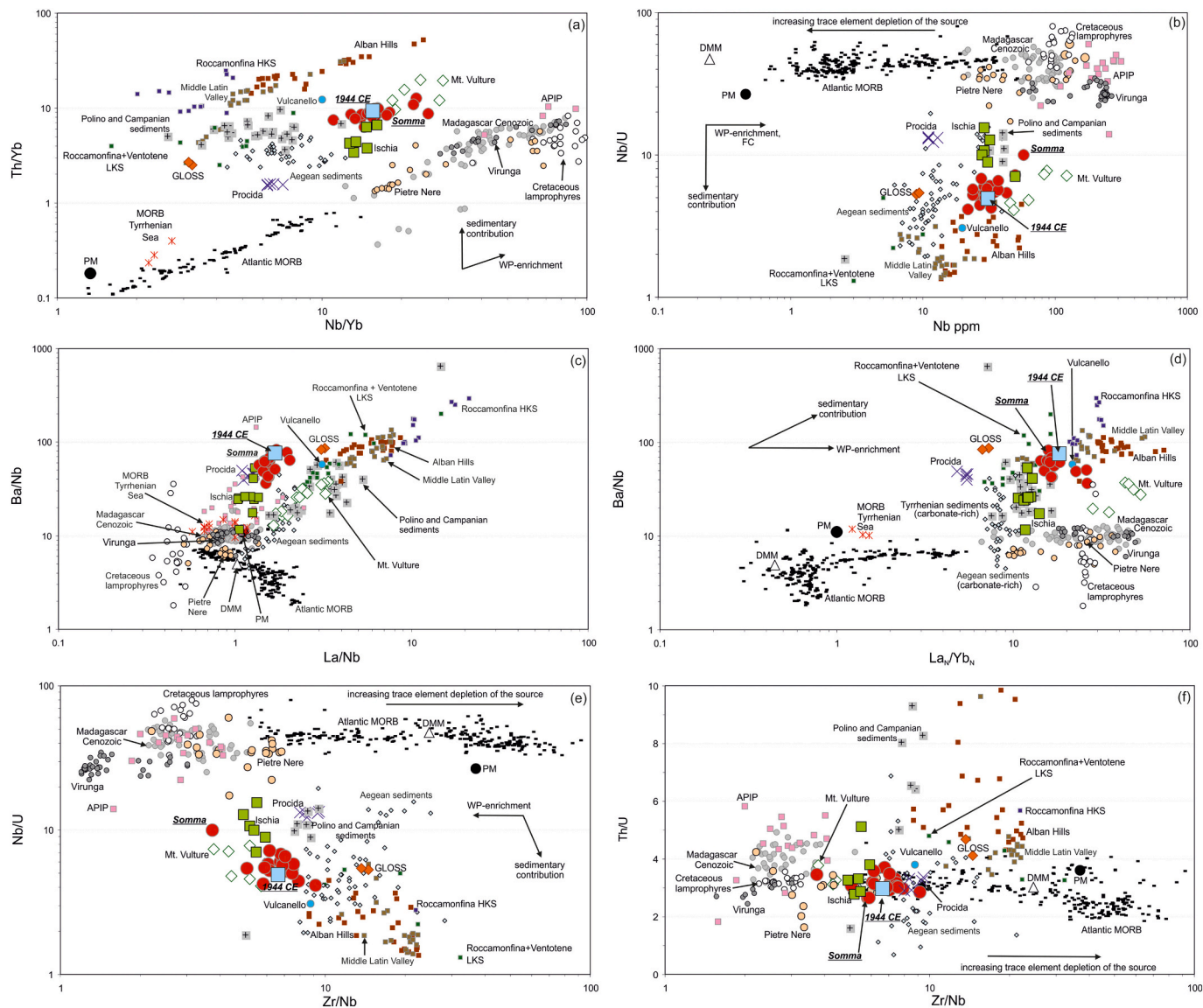


Fig. 5. (a-b) Nb/Yb vs. Th/Yb and Nb ppm vs. Nb/U; (c-d) La/Nb vs. Ba/Nb and La_N/Yb_N vs. Ba/Nb (e-f) Zr/Nb vs. Nb/U and Th/U diagrams for Mt. Somma lavas and dikes and lava of 1944 CE. The data used for comparison comes from the following references: Arevalo and McDonough (2010); Balassone et al. (2016); Belkin et al. (1993); Beccaluva et al. (1990, 1991, 2002); Boari et al. (2009a, 2009b); Conticelli et al. (2009a, b, 2015); D'Antonio et al. (1999); Mazzeo et al. (2014, 2018); Melluso et al. (2012, 2014, 2016); Plank and Langmuir (1998); Stoppa et al. (2014); Avanzinelli et al. (2018); Woelki et al. (2018); Klaver et al. (2015); Lustrino et al. (2012); Guarino et al. (2013); Fedele et al. (2008); De Astis et al. (2006); Minissale et al. (2022).

% removal of a leucite-rich extract (~46–55 wt% leucite, ~22–29 wt% clinopyroxene, ~10–14 wt% plagioclase, ~2–3 wt% olivine, ~5–7 wt% magnetite, and ~3–4 wt% apatite; $\Sigma R^2 = 0.097\text{--}0.239$). In the MSU group, the transition from the least to the most evolved lava compositions of the mildly silica undersaturated rocks (from MRL100 or MRL27 to MRL86 samples) was adequately modeled with 21–32 % removal of similar clinopyroxene-rich leucite gabbro (essexite) solid (~43–45 wt% clinopyroxene, ~27–38 wt% leucite, ~2–16 wt% plagioclase, ~7 wt% olivine, ~5–8 wt% magnetite, and ~0–2 wt% apatite; $\Sigma R^2 = 0.03\text{--}0.08$). The transition from less evolved “shoshonitic” MSU samples (i.e., MRL100 and MRL27) to more evolved latites (samples MRL103 and MRL104) is obtained by 40–56 % removal of a leucite-bearing clinopyroxenite (~37–41 wt% clinopyroxene, ~23–33 wt% leucite, ~13–21 wt% plagioclase, ~6–9 wt% olivine, ~1–3 wt% apatite, and ~5–7 wt% magnetite; at $\Sigma R^2 = 0.12\text{--}0.18$). The transition to the most evolved latites (from sample MRL69 to sample MRL104) is compatible with a 26 % removal of a clinopyroxene- and leucite-rich gabbro (~59 wt% plagioclase, ~25 wt% clinopyroxene, ~5 wt% leucite, ~7 wt% olivine,

and ~3 wt% magnetite; $\Sigma R^2 = 0.20$).

The reliability of the major element mass balance calculations reported above is not a proof of the actual occurrence of a given process, but it is a strong indication of the reliability of processes involving the physical removal of phase assemblages with the chemical composition of the observed phenocrysts in an alkaline magmatic system. The amount of plagioclase removal in the different transitions is consistent with Sr being a weakly incompatible element, since a typical K_d for bytownitic/labradoritic plagioclase is close to 2 (e.g., Bedard, 2006).

6.3. Modeling the transition from leucite-bearing shoshonitic to leucite-tephritic magmas

We have shown that the major and trace element variations of the most primitive magmas of each group of rocks recognized within the Mt. Somma activity cannot be produced by closed system fractional crystallization processes involving mineralogical assemblages represented by the phenocrysts (and their compositions) observed in the thin

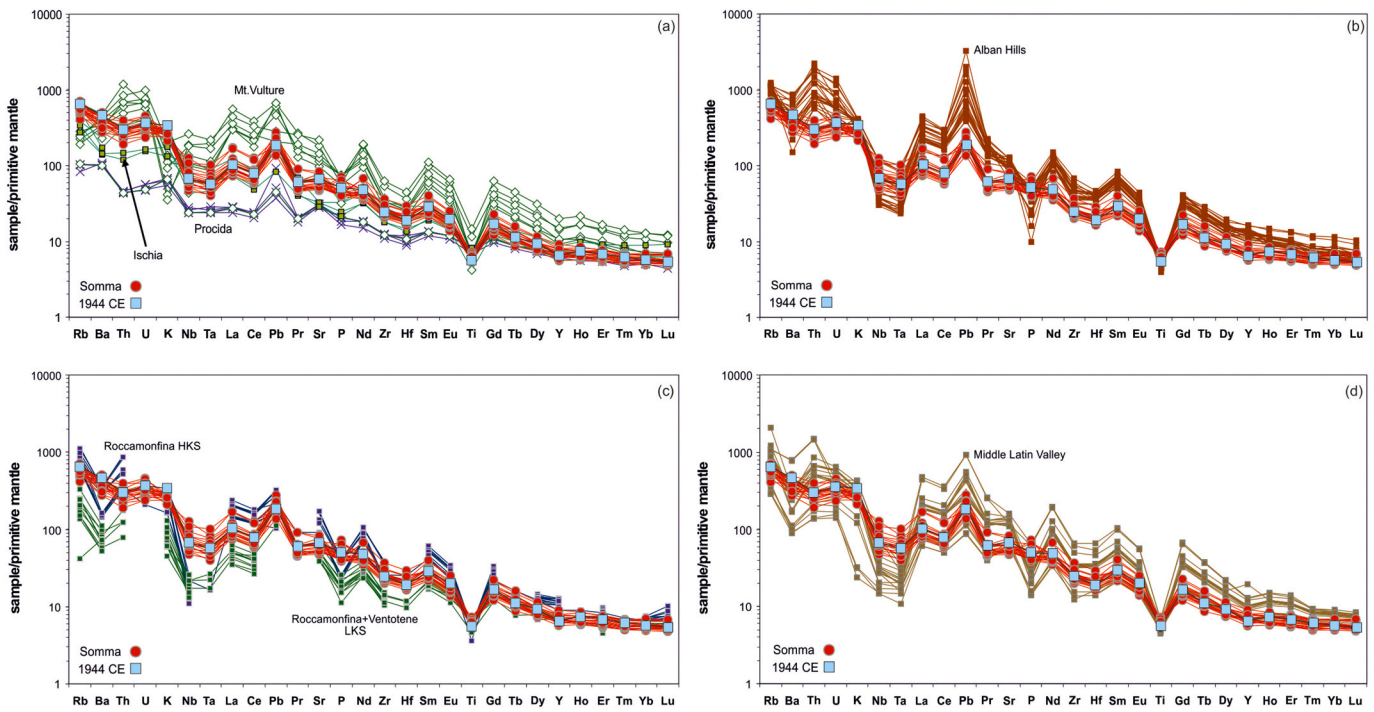


Fig. 6. Mantle-normalized multielement patterns for Monte Somma lavas and dikes and lava of 1944 CE compared with Mt. Vulture, Procida, Alban Hills, Roccamonfina, Ventotene, and Middle Latin Valley rocks (Beccaluva et al., 1991, 2002; Boari et al., 2009a, 2009b; Conticelli et al., 2009b; De Astis et al., 2006). The normalization values are from Lyubetskaya and Korenaga (2007).

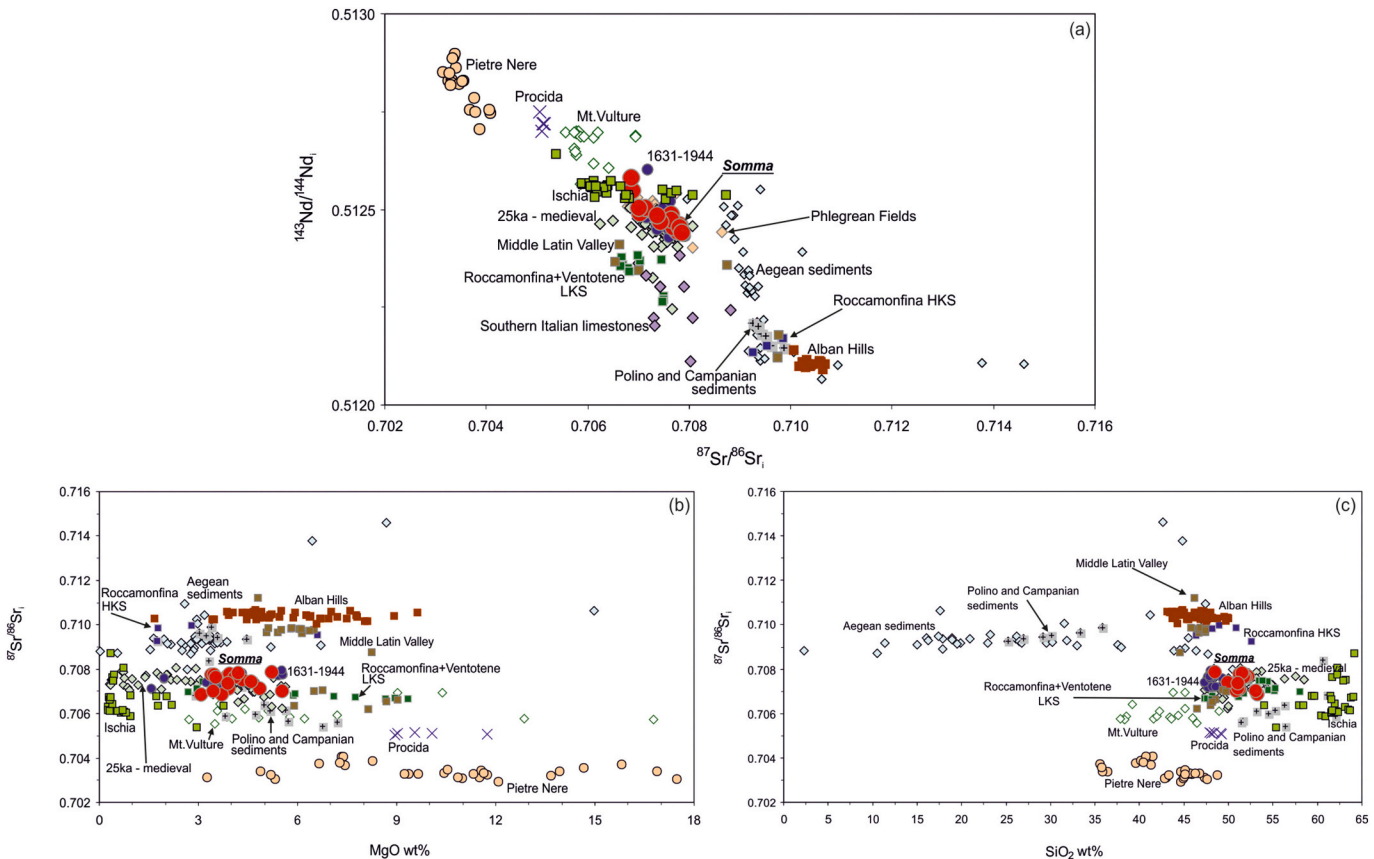


Fig. 7. $^{87}\text{Sr}/^{86}\text{Sr}$ vs. $^{143}\text{Nd}/^{144}\text{Nd}$ and $^{87}\text{Sr}/^{86}\text{Sr}$ vs. SiO₂ and MgO diagrams for the Somma rocks. The data used for comparison are from the following references: D'Antonio and Di Girolamo (1994); D'Antonio et al. (1996, 1999, 2007); Mazzeo et al. (2014, 2018); Conticelli et al. (1997, 2002, 2007); Ayuso et al. (1998); De Astis et al. (2006); Pappalardo et al. (2002); Peccerillo (2005) and references therein; Boari et al. (2009a, 2009b); Casalini et al. (2018); Rosatelli et al. (2023).

Table 2

Oxygen isotopes on olivines and clinopyroxenes separated from the most representative Mt. Somma samples.

	Sample	Type	$\delta^{18}\text{O}/^{16}\text{O}_{\text{ol}} (\text{\textperthousand})$	$\delta^{18}\text{O}/^{16}\text{O}_{\text{cpx}} (\text{\textperthousand})$
SSU group	MRL19	Lava	7.25	
	MRL82	Lava	7.38	
MSU group	MRL59	Lava	6.51	6.47
	MRL21	Lava	7.20	6.81
	MRL100	Lava	6.77	7.02
	MRL23	Lava	6.56	6.76
	MRL24	Dyke	6.83	6.31
	MRL27	Lava	6.86	6.83
	MRL38	Lava	6.39	6.55
	MRL37	Lava		7.04
	MRL7	Lava		6.77
	MRL93	Dyke		6.81
Latite group	MRL48	Lava	6.99	
	MRL51	Lava	6.69	6.66
	MRL103	Lava		7.90

sections. Petrographic (e.g., variably zoned plagioclase and clinopyroxene phenocrysts, the occurrence of skarn and limestone xenoliths) and petrochemical evidence (chemical disequilibrium between clinopyroxene crystals and their host bulk-rock composition, pronounced scatter of major and trace element concentrations, isotopic variability within juvenile clasts from the same eruption) seem to suggest the occurrence of open-system fractional crystallization (e.g., Santacroce, 1987; Ayuso

et al., 1998; Peccerillo, 2005; Piochi et al., 2006; Di Renzo et al., 2007).

Simple Assimilation and Fractional Crystallization (AFC; DePaolo, 1981) models were performed to reproduce the transition from weakly silica undersaturated Somma-Vesuvius magmas to mildly and strongly silica undersaturated magmas using limestone compositions as contaminants. Trace element and isotope modeling failed to reproduce such a transition, even with different contaminants, such as marls and limestones belonging to the Apennine chain (Fig. 8b, c). The close correlation of the Mt. Somma rocks with a marl-type contamination versus a limestone-type contamination is well illustrated by these models (Fig. 8b, c).

The very low incompatible element concentrations of the limestones (e.g., Rb ~2–4 ppm, Zr <26 ppm, La ~15 ppm, Nd ~10 ppm, Eu ~0.38 ppm, Tb ~0.9 ppm, Th <3 ppm, e.g., Zhang et al., 2017; Rosatelli et al., 2023) would result in a significant decrease in the incompatible element concentrations of the “hybridized” strongly silica undersaturated magma, which is contro-balanced by fractional crystallization.

However, the moderate variability of the Sr—Nd isotope ratios is consistent with the interaction of Somma-Vesuvius magmas with wall rock compositions that do not exhibit markedly different isotopic values, as in the case of typical Mesozoic limestones/dolostones of the Apennine chain ($^{87}\text{Sr}/^{86}\text{Sr} \sim 0.707$ –0.709 and $^{143}\text{Nd}/^{144}\text{Nd} \sim 0.512$; Del Muro et al., 2001; Melluso et al., 2003; Fulignati et al., 2005; Piochi et al., 2006; Conticelli et al., 2009a, 2009b; Boari et al., 2009b; Rosatelli et al., 2023), which is one of the rock types in the basement beneath the Somma-Vesuvius area (e.g., Santacroce, 1987; Brocchini et al., 2001).

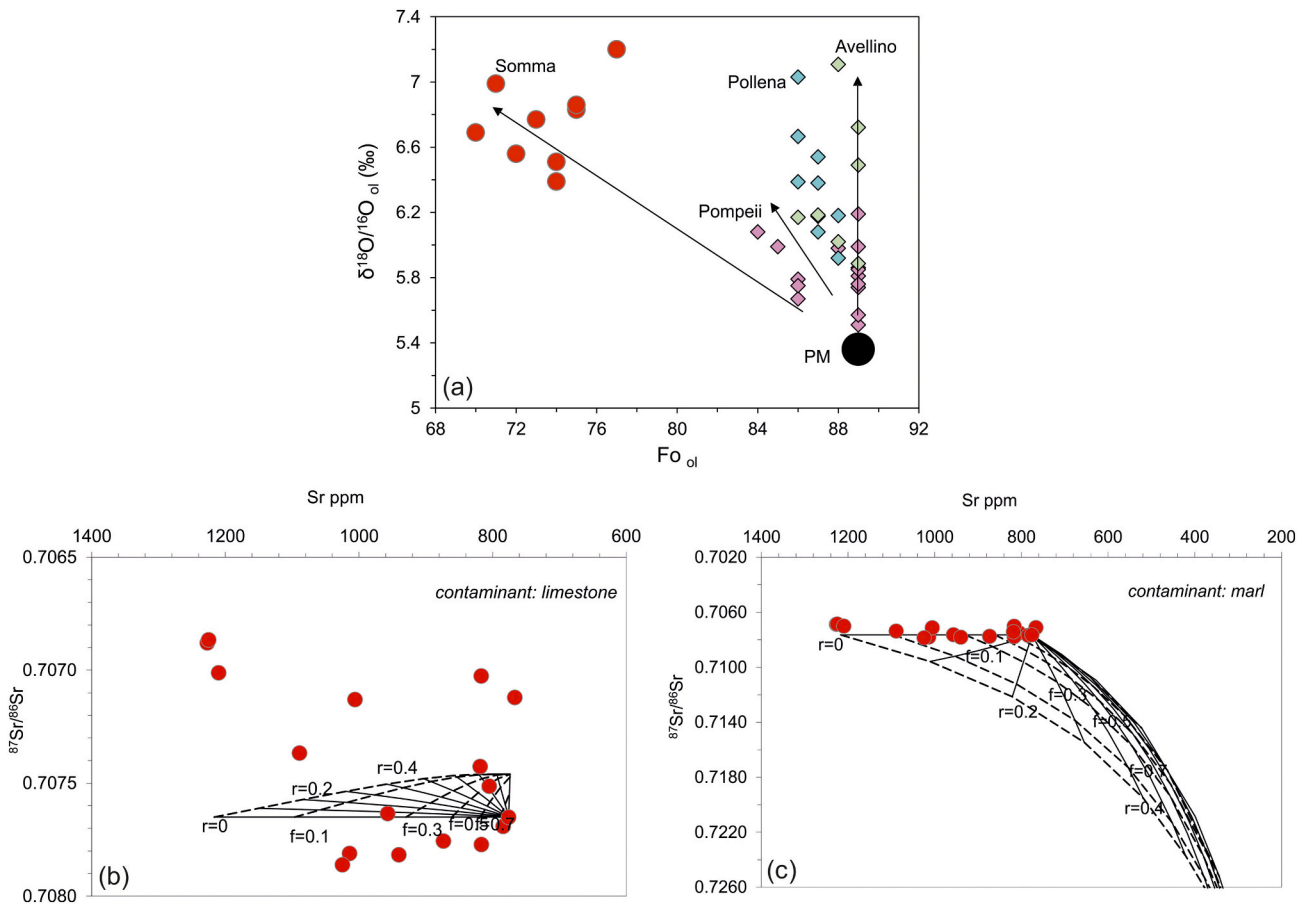


Fig. 8. (a) The forsterite - $\delta^{18}\text{O}_{\text{ol}}$ covariation trend can be used to compare the unevolved lavas from Mt. Somma and Mt. Vesuvius magmatic activity with respect to their degree of interaction with crustal CO_2 before/during differentiation. As the MgO decreases, the differentiation proceeds and the $\delta^{18}\text{O}$ values increase, indicating a higher degree of carbonate contamination. The stability of olivine likely indicates the presence of dolomitic carbonate in the assimilated material. (b, c) Assimilation and Fractional Crystallization (AFC) model (DePaolo, 1981) assuming the most primitive lava of this study and limestone and marl contaminants, as representative of the basement beneath Somma-Vesuvius.

In summary, the above evidence and modeling indicate that the process of limestone assimilation was active throughout the magmatic evolution of the Somma-Vesuvius complex, but it is not able to justify the observed temporal increase in the degree of alkalinity and silica undersaturation of these magmas, also considering the variations of $\delta^{18}\text{O}$ in the Mt. Somma (and Vesuvius) magmas and the isotopic differences between ultrapotassic alkaline magmas and sedimentary limestones/dolostones or marlstones (e.g., Dallai et al., 2019; Fan et al., 2021; Rosatelli et al., 2023).

6.4. The mantle sources of the Somma-Vesuvius magmatism in the southern part of the Roman Magmatic Province

It is widely accepted that the primary magmas of the RMP were generated by partial melting of a mantle source recently enriched in potassium and related elements by subduction processes involving continental crustal material (e.g., Beccaluva et al., 1991; Conticelli and Peccerillo, 1992; Peccerillo, 1998, 2017; Conticelli et al., 2002, 2011, 2015a; Avanzinelli et al., 2008, 2009; Mazzeo et al., 2014; Iovine et al., 2018; Casalini et al., 2019). The relative roles of subducted sedimentary material in a variably enriched lithospheric upper mantle and shallow crustal contamination en route to the surface are still debated. The typical LILE and Pb enrichments and the troughs at Nb, Ta, and Ti observed in the most primitive mantle-normalized diagrams for the Mt. Somma ones are shared with other Roman volcanic rocks, although the Mt. Somma volcanic rocks have intermediate characteristics between leucite-bearing volcanic rocks of the Latian district and those of Mt. Vulture (e.g., Avanzinelli et al., 2009; Conticelli et al., 2015a, 2015b). The mafic terms of the Somma-Vesuvius and other volcanoes of the Campanian Plain have lower HFSE fractionation than Th, U and LILE compared to the leucite-bearing mafic magmas of the Latian districts of the Roman Province (e.g., Beccaluva et al., 1991; Ayuso et al., 1998; D'Antonio et al., 1999; Peccerillo, 2001; Di Renzo et al., 2007; Avanzinelli et al., 2008, 2009; Conticelli et al., 2009a; Mazzeo et al., 2014).

It has long been known that the extent of the Eu troughs in the REE chondrite normalized diagrams of the mafic ultrapotassic, leucite-bearing rocks of the RMP is a feature largely inherited from an anomalous mantle source, rather than due to low-pressure removal of calcic plagioclase (e.g., Rogers et al., 1985); the Mt. Somma lavas (and the Vesuvius analogues) are no exception. The source of the RMP rocks has marked affinities with sedimentary rocks (pelites with carbonates/marls), and indeed the addition of pelitic sedimentary rocks (or melts derived from them) in a peridotite matrix could be one of the causes of the geochemical patterns of the RMP and hence of Somma-Vesuvius. To test this hypothesis, we have used a comprehensive data set of the Italian volcanic rocks south of the Alban Hills, together with the composition of typical Atlantic and Tyrrenian Sea MORBs, within plate basalts, and sedimentary rocks of closed areas, thought to be representative of the subducted material potentially downdragged during the Cenozoic collisional events of this area of the Apennine chain. The Nb/Yb vs. Th/Yb and Nb vs. Nb/U plots point out significant differences between the regional geochemistry of MORB and within-plate mafic rocks, and that of Mt. Somma and the other volcanic rocks of the southern RMP (Fig. 5a, b). The shift to high Th/Yb and lower Nb/U compared to the MORB-WPB array indicates a differential enrichment in Th and U, at different Nb concentrations, which may be related to the degree of "within-plate" enrichment. The latter indicates the effect of fractional crystallization, but also the degree of HFSE enrichment in the mantle source, which is highest for alkaline WPB around the RMP, such as Pietre Nere, Capo Passero (Avanzinelli et al., 2012; Mazzeo et al., 2018), Cretaceous within-plate lamprophyres of the Apennine chain (Stoppa et al., 2014), and other within plate potassic or sodic provinces (such as Madagascar, Virunga, and southeastern Brazil; cf. Guarino et al., 2013; Minissale et al., 2022). The mafic rocks of Ischia, Procida, Phleorean Fields, and Somma-Vesuvius, although having a markedly distinct composition, are also different from the rocks of the potassic-ultrapotassic volcanic rocks

from Roccamonfina to the Alban Hills. There is another interesting aspect related to the different genesis and geochemistry of the Pre-Miocene Apennine magmatism and the post-Miocene magmatism of the Tyrrenian Sea margin, which implies that the K-enrichment of the sources is recent and not related to an older (i.e., Hercynian, Late Paleozoic) collisional event (e.g., Gaeta et al., 2016), where also potassic silica-undersaturated magmatism is exceedingly rare. The La/Nb vs. Ba/Nb and La_N/Yb_N vs. Ba/Nb plots highlight that the mafic rocks of the Campanian district plot differently from the rest of the RMP rocks, being displaced at higher Ba/Nb for a given La/Nb (Fig. 5c, d). The shift almost disappears when the REE fractionation is considered, with only the composition of MORB and WPB being significantly different.

The Zr/Nb vs. Nb/U and Zr/Nb vs. Th/U plots also highlight peculiar aspects of the selective elemental enrichment of the Italian volcanic rocks (Fig. 5e, f): the displacement of the potassic-ultrapotassic rocks from the MORB-WPB trend is the largest at high Zr/Hf, with the largest U enrichment found in the Alban Hills, Roccamonfina and Middle Latin Valley, and the markedly higher Th/U ratios of the Roccamonfina, Alban Hills and Middle Latin Valley rocks compared to those of the Campanian volcanoes, including Somma-Vesuvius. The type of sediment addition provides evidence that adding bulk compositions of the sedimentary rocks (e.g., Klaver et al., 2015; Balassone et al., 2016; Zhang et al., 2017; Woelki et al., 2018) are not in the highest Ba/Nb and La/Nb field of the diagrams and thus do not fully reproduce the trend, suggesting that sediment-derived fluids and melts, rather than direct sediment addition, were the components that metasomatized the mantle source and imparted the potassic.ultrapotassic signature to the magmas. Compared to other silica-undersaturated ultrapotassic magmas of the Latian district, those of Somma-Vesuvius and those of the other Neapolitan volcanoes have significantly lower $^{87}\text{Sr}/^{86}\text{Sr}$, and higher $^{143}\text{Nd}/^{144}\text{Nd}$ and $^{206}\text{Pb}/^{204}\text{Pb}$ (e.g., Conticelli et al., 2002, 2007, 2010, 2015a and references therein; Di Renzo et al., 2007). In turn, the peculiar composition of the radiogenic isotope systematics is again attributed to the recycling of carbonate-bearing crustal materials (e.g., Avanzinelli et al., 2009; Conticelli et al., 2010, 2015a, 2015b). The involvement of such materials has been demonstrated by cross-checking different geochemical tools. The evidence provided by U-series and non-traditional stable isotopes (Mo and U) suggests that although limestone assimilation could potentially occur and influence major element concentrations, the same process is not able to significantly affect the isotopic composition and the elemental abundances of Vesuvius rocks (Avanzinelli et al., 2018; Casalini et al., 2019). On the other hand, partial melting experiments on carbonate-rich sediments at subarc conditions (P-T) may indicate that the stabilization of phases, such as epidote, influences the geochemical budget of the mantle source and, consequently, of subduction-derived products (e.g., Skora et al., 2015). In the case of Somma-Vesuvius, the presence of residual epidote during the partial melting of subducted Ca-rich sediments could explain the formation of magmas enriched in U over Th (but also in the relative proportions of other trace elements, such as Ce and Mo) and with the typical signature of both radiogenic and stable isotopes (i.e., ^{238}U -excess, $\delta^{238}\text{U}$, $\delta^{98}\text{Mo}$; Avanzinelli et al., 2018; Casalini et al., 2019). In this context, the lithological control of the metasediments involved in the ultimate petrogenesis of the magmas in the southern part of the RMP is an important parameter to consider.

The geochemical and isotopic comparison of the Mt. Somma lavas with the mafic products of the neighboring volcanoes (the Solchiaro basalts of Procida, the Grotta di Terra dyke and Arso lava, and the Zaro mafic inclusions of Ischia) is reported in the Figs. 4, 6 and 7. Two main aspects are there highlighted: (1) the imprint of crustal materials in the mantle source of the Ischian and Phleorean magmas is much less pronounced than in the source of the Mt. Somma magmas; (2) the mantle sources of the Campanian volcanic district are to be considered isotopically and geochemically heterogeneous and only generally the result of the same petrogenetic processes in a post-collisional tectonic setting.

7. Conclusions

The Mt. Somma stratovolcano, which represent the first stage of the Somma-Vesuvius volcanic complex, is characterized dominantly by lavas of leucite-bearing to shoshonite compositions, although significantly less silica undersaturated than the recent Vesuvius (s.s.) Great Cone volcanic rocks at the same level of differentiation. The Mt. Somma volcanic rocks are generally characterized by a differentiated composition. Petrographic differences observed in the different magma groups are not reflected in the geochemistry and Sr-Nd-O isotopic compositions, which overlap. Crustal contamination en route to the surface, in particular interaction with the carbonate lithologies beneath Somma-Vesuvius, is shown to be widespread in the skarn xenoliths occurring in the Vesuvius (s.s.) volcanic rocks, but the subduction-related trace element signature of the Mt. Somma lavas (as well as the younger Vesuvius lavas) argues for a dominant role of deep sedimentary contamination in the mantle source prior to partial melting. This is a geologically recent feature acquired in a moderately enriched mantle source, more limited in extent when compared to the strongly sediment-modified mantle in the Latian districts (Northern Roman Magmatic Province). The leucite-bearing Mt. Somma lavas have very little in common with the rocks belonging to the neighboring volcanic areas (Ischia, Procida and Phleorean Fields), confirming once again the geochemical characteristics of independent feeding systems, liquid lines of descent and periods of activity.

Supplementary data to this article can be found online at <https://doi.org/10.1016/j.chemer.2023.126076>.

CRediT authorship contribution statement

Vincenza Guarino: Conceptualization, Methodology, Software, Validation, Formal analysis, Investigation, Resources, Data curation, Writing – original draft, Writing – review & editing, Visualization, Supervision, Funding acquisition, Project administration. **Roberto Solone:** Conceptualization, Formal analysis, Visualization. **Martina Casalini:** Methodology, Software, Validation, Formal analysis, Investigation, Resources, Data curation, Writing – original draft, Writing – review & editing, Visualization, Funding acquisition. **Luigi Franciosi:** Formal analysis, Writing – review & editing, Visualization. **Luigi Dallai:** Methodology, Validation, Formal analysis, Investigation, Resources, Data curation, Writing – original draft, Writing – review & editing, Visualization, Funding acquisition. **Vincenzo Morra:** Validation, Writing – review & editing, Visualization, Supervision. **Sandro Conticelli:** Conceptualization, Software, Validation, Investigation, Resources, Writing – original draft, Writing – review & editing, Visualization, Supervision, Funding acquisition, Project administration. **Leone Melluso:** Conceptualization, Validation, Formal analysis, Investigation, Resources, Writing – original draft, Writing – review & editing, Visualization, Supervision, Funding acquisition, Project administration.

Declaration of competing interest

The authors declare that they have no known competing financial interests or personal relationships that could have appeared to influence the work reported in this paper.

Acknowledgements

This manuscript is dedicated to the memory of Prof. Pio Di Girolamo, for his never-ending passion for the rocks of Somma-Vesuvius and for his precious teaching on the genesis of Italian potassian and ultrapotassian magmas. We are particularly grateful to Lorenzo Fedele for his help in the study of these samples, Ciro Cucciniello for the XRF analyses and useful advice, and Roberto de Gennaro for the microprobe work. Mariano Mercurio helped with the collection of samples during the R.S. MSc thesis. Fabio Mazzeo, Pietro Armienti and Giancarlo Serri are also

in our souls. Sergio Bravi patiently prepared polished thin sections. This work was supported by MIUR 2015 grants to LM and SC (grants # 2015A9CBM, 20224T2JF4) and by MIUR 2017 grant to Ciro Cucciniello (grant # 2017LPCPW_004) and Fondi Ricerca Dipartimentale 2022 and 2023 to V.G., L.M., and M.C. The authors would like to thank the Astrid Holzheid, Editor-in-Chief of Geochemistry, and the constructive comments of Rajesh Srivastava and two anonymous reviewers, which were very useful in the preparation of this revised manuscript.

References

- Anders, E., Grevesse, N., 1989. Abundances of the elements: meteoritic and solar. *Geochim. Cosmochim. Acta* 53, 197–214.
- Arevalo, R., McDonough, W.F., 2010. Chemical variations and regional diversity observed in MORB. *Chem. Geol.* 271, 70–85.
- Avanzinelli, R., Boari, E., Conticelli, S., Francalanci, L., Guarneri, L., Perini, G., Petrone, C.M., Tommasini, S., Uliivi, M., 2005. High precision Sr, Nd, and Pb isotopic analyses and reproducibility using new generation thermal ionisation mass spectrometer: aims and perspective for isotope geology applications. *Period. Mineral.* 74, 147–166.
- Avanzinelli, R., Elliott, T., Tommasini, S., Conticelli, S., 2008. Constraints on the genesis of the potassium-rich Italian volcanics from U/Th disequilibrium. *J. Petrol.* 49, 195–223.
- Avanzinelli, R., Lustrino, M., Mattei, M., Melluso, L., Conticelli, S., 2009. Potassian and ultrapotassian magmatism in the circum-Tyrrhenian region: the role of carbonated pelitic vs. pelitic sediment recycling at destructive plate margin. *Lithos* 113, 213–227.
- Avanzinelli, R., Sapienza, G.T., Conticelli, S., 2012. The cretaceous to Paleogene within-plate magmatism of Pachino-capo Passero (southeastern Sicily) and Adria (La Queglia and Pietre Nere, southern Italy): geochemical and isotopic evidence against a plume-related origin of circum-Mediterranean magmas. *Eur. J. Mineral.* 24, 73–96.
- Avanzinelli, R., Cioni, R., Conticelli, S., Giordano, G., Isaia, R., Mattei, M., Melluso, L., Sulpizio, R., 2017. The Vesuvius and the other volcanoes of Central Italy. *Geol. Field Trips Maps* 9, No.1.1. <https://doi.org/10.3301/GFT.2017.01>, 158 pp.
- Avanzinelli, R., Casalini, M., Elliott, T., Conticelli, S., 2018. Carbon fluxes from subducted carbonates revealed by uranium excess at Mount Vesuvius, Italy. *Geology* 46, 259–262. <https://doi.org/10.1130/G39766.1>.
- Avanzinelli, R., Bianchini, G., Tiepolo, M., Jasim, A., Natali, C., Braschi, E., Conticelli, Beccaluva, L., 2020. Subduction-related hybridization of the lithospheric mantle revealed by trace element and Sr-Nd-Pb isotopic data in composite xenoliths from Tallante (Betic cordillera, Spain). *Lithos* 352, 105316.
- Ayuso, A.R., De Vivo, B., Rolandi, G., Seal, R.R., Paone, A., 1998. Geochemical and isotopic (Nd-Pb-Sr-O) variations bearing on the genesis of volcanic rocks from Vesuvius, Italy. *J. Volcanol. Geotherm. Res.* 82, 53–78.
- Balassone, G., Scordari, F., Lacalamita, M., Schingaro, E., Mormone, A., Piochi, M., Petti, C., Mondillo, N., 2013. Trioctahedral micas in xenolithic ejecta from recent volcanism of the Somma-Vesuvius (Italy): crystal chemistry and genetic inferences. *Lithos* 160, 84–97.
- Balassone, G., Aiello, G., Barra, D., Cappelletti, P., De Bonis, A., Donadio, C., Guida, M., Melluso, L., Morra, V., Parisi, R., Pennetta, M., Siciliano, A., 2016. Effects of anthropogenic activities in a Mediterranean coastal: the case study of the Falerno-Domitio littoral in Campania, Tyrrhenian Sea (southern Italy). *Mar. Pollut. Bull.* 112, 271–290.
- Balassone, G., Schingaro, E., Lacalamita, M., Mesto, E., Mormone, A., Piochi, M., Guarino, V., Pellino, A., D’Orazio, L., 2023. Genetic implications, composition, and structure of trioctahedral micas in xenoliths related to Plinian eruptions from the Somma-Vesuvius volcano (Italy). *Am. Mineral.* in press, doi: <https://doi.org/10.2138/am-2022-8782>.
- Beccaluva, L., Bonatti, E., Dupuy, C., Ferrara, G., Innocenti, F., Lucchini, F., Macera, P., Petrini, R., Rossi, P.L., Serri, G., Seyler, M., Siena, F., 1990. Geochemistry and mineralogy of volcanic rocks from ODP sites 650, 651, 655 and 654 in the Tyrrhenian Sea. In: Proceedings of the Ocean Drilling Program Scientific Results, 107, pp. 49–74.
- Beccaluva, L., Di Girolamo, P., Serri, G., 1991. Petrogenesis and tectonic setting of the Roman Volcanic Province, Italy. *Lithos* 26, 191–221.
- Beccaluva, L., Coltorti, M., Di Girolamo, P., Melluso, L., Milani, L., Morra, V., Siena, F., 2002. Petrogenesis and evolution of Mt. Vulture alkaline volcanism (southern Italy). *Mineral. Petrol.* 74, 277–297.
- Bedard, J.H., 2006. Trace element partitioning in plagioclase feldspar. *Geochim. Cosmochim. Acta* 70, 3717–3742.
- Belkin, H.E., Kilburn, C.R., de Vivo, B., 1993. Sampling and major element chemistry of the recent (AD 1631–1944) Vesuvius activity. *J. Volcanol. Geotherm. Res.* 58 (1–4), 273–290.
- Boari, E., Avanzinelli, R., Melluso, L., Giordano, G., Mattei, M., De Benedetti, A.A., Morra, V., Conticelli, S., 2009a. Isotope geochemistry (Sr-Nd-Pb) and petrogenesis of leucite-bearing volcanic rocks from “Colli Albani” volcano, Roman Magmatic Province, Central Italy: inferences on volcano evolution and magma genesis. *Bull. Volcanol.* 71, 977–1005.
- Boari, E., Tommasini, S., Laurenzi, M.A., Conticelli, S., 2009b. Transition from ultrapotassian kamafugitic to sub-alkaline magmas: Sr, Nd, and Pb isotope, trace

- element and ^{40}Ar - ^{39}Ar age data from the middle Latin Valley volcanic field, Roman Magmatic Province, Central Italy. *J. Petrol.* 50, 1327–1357.
- Bragagni, A., Mastrianni, F., Münker, C., Conticelli, S., Avanzinelli, R., 2022. A carbon-rich lithospheric mantle as a source for the large CO₂ emissions of Etna volcano (Italy). *Geology* 50, 486–490.
- Brocchini, D., Principe, C., Castradori, D., Laurenzi, M.A., Gorla, L., 2001. Quaternary evolution of the southern sector of the Campanian Plain and early Somma-Vesuvius activity: insights from the Trecase I well. *Mineral. Petrol.* 73, 67–91.
- Carter, L.B., Dasgupta, R., 2016. Effect of melt composition on crustal carbonate assimilation: implications for the transition from calcite consumption to skarnification and associated CO₂ degassing. *Geochem. Geophys. Geosyst.* 17 (10), 3893–3916.
- Casalini, M., Heumann, A., Marchionni, S., Conticelli, S., Avanzinelli, R., Tommasini, S., 2018. Inverse modelling to unravel the radiogenic isotope signature of mantle sources from evolved magmas: the case-study of Ischia volcano. *Ital. J. Geosci.* 137. <https://doi.org/10.3301/IJG.2018.05>.
- Casalini, M., Avanzinelli, R., Tommasini, S., Elliott, T., Conticelli, S., 2019. Ce/Mo and molybdenum isotope systematics in subduction-related orogenic potassic magmas of central-southern Italy. *Geochim. Geophys. Geosystems* 20, 2753–2768.
- Chen, L.M., Song, X.Y., Hu, R.Z., Yu, S.Y., Yi, J.N., Kang, J., Huang, K.J., 2021. Mg-Sr-Nd isotopic insights into Petrogenesis of the Xiarihamu mafic-ultramafic intrusion, northern Tibetan plateau, China. *J. Petrol.* 62 (2), egaa113.
- Chen, M., Boyle, E.A., Jiang, S., Liu, Q., Zhang, J., Wang, X., Zhou, K., 2023. Dissolved lead (Pb) concentrations and Pb isotope ratios along the East China Sea and Kuroshio transect—evidence for isopycnal transport and particle exchange. *J. Geophys. Res. Oceans* 128 (2), e2022JC019423.
- Chiba, H., Chacko, T., Clayton, R.N., Goldsmith, J.R., 1989. Oxygen isotope fractionations involving diopside, forsterite, magnetite, and calcite: applications to geothermometry. *Geochim. Cosmochim. Acta* 53, 2985–2995.
- Cioni, R., Marianelli, P., Santacroce, R., 1998. Thermal and compositional evolution of the shallow magma chambers of Vesuvius: evidence from pyroxene phenocrysts and melt inclusions. *J. Geophys. Res. Solid Earth* 103 (B8), 18277–18294.
- Cioni, R., Santacroce, R., Sbrana, A., 1999. Pyroclastic deposits as a guide for reconstructing the multi-stage evolution of the Somma-Vesuvius caldera. *Bull. Volcanol.* 61, 207–222.
- Cioni, R., Bertagnini, A., Santacroce, R., Andronico, D., 2008. Explosive activity and eruption scenarios at Somma-Vesuvius (Italy): towards a new classification scheme. *J. Volcanol. Geother. Res.* 178, 331–346.
- Cioni, R., Isaia, R., Sulpizio, R., de Vita, S., Di Vito, M.A., Pistolesi, M., et al., 2019. The city of Napoli and its active volcanoes. *Geol. Field Trips Maps* 11 (1), 2.
- Conticelli, S., Peccerillo, A., 1992. Potassic and ultrapotassic volcanism from central Italy: compositional characteristics, petrogenesis and inferences on the evolution of the mantle source. *Lithos* 28, 221–240. [https://doi.org/10.1016/0024-4937\(92\)90008-M](https://doi.org/10.1016/0024-4937(92)90008-M).
- Conticelli, S., Franchalanci, L., Manetti, P., Cioni, R., Sbrana, A., 1997. Petrology and geochemistry of the ultrapotassic rocks from the Sabatini Volcanic District, Central Italy: the role of evolutionary processes in the genesis of variably enriched alkaline magmas. *J. Volcanol. Geotherm. Res.* 75, 107–136.
- Conticelli, S., D'Antonio, M., Pinarelli, L., Civetta, L., 2002. Source contamination and mantle heterogeneity in the genesis of Italian potassic and ultrapotassic volcanic rocks: Sr-Nd-Pb isotope data from Roman Province and southern Tuscany. *Mineral. Petrol.* 74, 189–222.
- Conticelli, S., Melluso, L., Avanzinelli, R., Perini, G., Boari, E., 2004. Petrologic and isotopic characteristics of potassic and ultrapotassic alkalic magmatism in central-southern Italy: inferences on its genesis and on the nature of its mantle source. *Period. Mineral.* 73, 135–164.
- Conticelli, S., Carlson, R.W., Widom, E., Serri, G., 2007. Chemical and isotopic composition (Os, Pb, Nd, and Sr) of Neogene to Quaternary calc-alkalic, shoshonitic, and ultrapotassic mafic rocks from the Italian peninsula: inferences on the nature of their mantle sources. In: G.S.A. Special Papers 'Cenozoic Volcanism in the Mediterranean Area', 418, p. 171. [https://doi.org/10.1130/2007.2418\(09\).1](https://doi.org/10.1130/2007.2418(09).1).
- Conticelli, S., Guarneri, L., Farinelli, A., Mattei, M., Avanzinelli, R., Bianchini, G., Boari, E., Tommasini, S., Tiepolo, M., Prelećević, D., Venturelli, G., 2009a. Trace elements and Sr-Nd-Pb isotopes of K-rich to shoshonitic and calc-alkalic magmatism of the Western Mediterranean region: genesis of ultrapotassic to calc-alkalic magmatic associations in post-collisional geodynamic setting. *Lithos* 107, 68–92.
- Conticelli, S., Marchionni, S., Rosa, D., Giordano, G., Boari, E., Avanzinelli, R., 2009b. Shoshonite and sub-alkaline magmas from an ultrapotassic volcano: Sr-Nd-Pb isotope data on the Roccamonfina volcanic rocks, Roman Magmatic Province, southern Italy. *Contrib. Mineral. Petrol.* 157, 41–63.
- Conticelli, S., Laurenzi, M.A., Giordano, G., Mattei, M., Avanzinelli, R., Melluso, L., Tommasini, S., Boari, E., Cifelli, F., Perini, G., 2010. Leucite-bearing (Kamafugitic/leucitic) and-free (lamproitic) ultrapotassic rocks and associated shoshonites from Italy: constraints on petrogenesis and geodynamics. *J. Virtual Explor.* 36 (20), 1–95.
- Conticelli, S., Avanzinelli, R., Marchionni, S., Tommasini, S., Melluso, L., 2011. Sr-Nd-Pb isotopes from the Radicofani Volcano, Central Italy: constraints on heterogeneities in a veined mantle responsible for the shift from ultrapotassic shoshonite to basaltic andesite magmas in a post-collisional setting. *Mineral. Petrol.* 103, 123–148.
- Conticelli, S., Avanzinelli, R., Poli, G., Braschi, E., Giordano, G., 2013. Shift from lamproite-like to leucitic rocks: Sr-Nd-Pb isotope data from the Monte Cimino volcanic complex vs. the Vico stratovolcano, Central Italy. *Chem. Geol.* 353, 246–266.
- Conticelli, S., Avanzinelli, R., Ammannati, E., Casalini, M., 2015a. The role of carbon from recycled sediments in the origin of ultrapotassic igneous rocks in the Central Mediterranean. *Lithos* 232, 174–196.
- Conticelli, S., Boari, E., Burlamacchi, L., Cifelli, F., Moscardi, F., Laurenzi, M.A., Ferrari Pedraglio, L., Franchalanci, L., Benvenuti, M.G., Braschi, E., Manetti, P., 2015b. Geochemistry and Sr-Nd-Pb isotopes of Monte Amiata Volcano, Central Italy: evidence for magma mixing between high-K calc-alkaline and leucitic mantle-derived magmas. *Ital. J. Geosci.* 134, 266–290. <https://doi.org/10.3301/IJG.2015.12>.
- Cucciniello, C., Melluso, L., le Roex, A.P., Jourdan, F., Morra, V., de' Gennaro, R., Grifa, C., 2017. From nepheline, basanite and basalt to peralkaline trachyphylonolite and comendite in the Ankaratra volcanic complex, Madagascar: ^{40}Ar - ^{39}Ar ages, phase compositions and bulk-rock geochemical and isotopic evolution. *Lithos* 274–275, 363–382. <https://doi.org/10.1016/j.lithos.2016.12.026>.
- Cucciniello, C., Avanzinelli, R., Sheth, H.C., Casalini, M., 2022. Mantle and crustal contributions to the Mount Girnar alkaline plutonic complex and the circum-Girnar mafic-silicic intrusions of Saurashtra, northwestern Deccan Traps. *J. Petrol.* 63, egac007. <https://doi.org/10.1093/petrology/egac007>.
- Dallai, L., Freda, C., Gaeta, M., 2004. Oxygen isotope geochemistry of pyroclastic clinopyroxene monitors carbonate contributions to Roman-type ultrapotassic magma. *Contrib. Mineral. Petrol.* 148, 247–263.
- Dallai, L., Cioni, R., Boschi, C., D'Oriano, C., 2011. Carbonate-derived CO₂ purging magma at depth: influence on the eruptive activity of Somma-Vesuvius, Italy. *Earth Planet. Sci. Lett.* 310, 84–95.
- Dallai, L., Bianchini, G., Avanzinelli, R., Natali, C., Conticelli, S., 2019. Heavy oxygen recycled into the lithospheric mantle. *Sci. Rep.* 9, 8793.
- Dallai, L., Bianchini, G., Avanzinelli, R., Deloule, E., Natali, C., Gaeta, M., Cavallo, A., Conticelli, S., 2022. Quartz-bearing rhyolitic melts in the Earth's mantle. *Nat. Commun.* 13 (1), 7765.
- D'Antonio, M., Di Girolamo, P., 1994. Petrological and geochemical study of mafic shoshonitic volcanics from Procida-Vivara and Ventotene Islands (Campanian region, South Italy). *Acta Vulcanol.* 5, 69–80.
- D'Antonio, M., Tilton, G.R., Civetta, L., 1996. Petrogenesis of Italian alkaline lavas deduced from Pb-Sr-Nd isotope relationships. In: Basu, A., Hart, S.R. (Eds.), *Earth Processes: Reading the Isotopic Code*, vol. 95. American Geophysical Union, Washington D.C., pp. 253–267. Monograph Series.
- D'Antonio, M., Civetta, L., Di Girolamo, P., 1999. Mantle source heterogeneity in the Campanian region (South Italy) as inferred from geochemical and isotopic features of mafic volcanic rocks with shoshonitic affinity. *Mineral. Petrol.* 67, 163–192.
- D'Antonio, M., Tonarini, S., Arienzo, I., Civetta, L., Di Renzo, V., 2007. Components and processes in the magma genesis of the Phlegraean Volcanic District, southern Italy. In: Beccaluva, L., Bianchini, G., Wilson, M. (Eds.), *Cenozoic Volcanism in the Mediterranean Area*. *Geol. Soc. Am. Spec. Pap.* vol. 418, pp. 203–220.
- De Astis, G., Kempton, P.D., Peccerillo, A., Wu, T.W., 2006. Trace element and isotopic variations from Mt. Vulture to Campanian volcanoes: constraints for slab detachment and mantle inflow beneath southern Italy. *Contrib. Mineral. Petrol.* 151, 331–351.
- de La Roche, H., Leterrier, P., Grandclaude, P., Marchal, E., 1980. A classification of volcanic and plutonic rocks using R₁-R₂ diagram and major element analyses. Its relationships with current nomenclature. *Chem. Geol.* 29, 183–210.
- Deegan, F.M., Troll, V.R., Freda, C., Misiti, V., Chadwick, J.P., McLeod, C.L., Davidson, J.P., 2010. Magma-carbonate interaction processes and associated CO₂ release at Merapi Volcano, Indonesia: insights from experimental petrology. *J. Petrol.* 51 (5), 1027–1051. <https://doi.org/10.1093/petrology/egg010>.
- Del Moro, A., Fulignati, P., Marianelli, P., Sbrana, A., 2001. Magma contamination by direct wall rock interaction: constraints from xenoliths from the walls of a carbonate-hosted magma chamber (Vesuvius 1944 eruption). *J. Volcanol. Geotherm. Res.* 112, 15–24.
- DePaolo, D.J., 1981. Trace element and isotopic effects of combined wall rock assimilation and fractional crystallization. *Earth Planet. Sci. Lett.* 53, 189–202.
- Di Girolamo, P., 1984. Magmatic character and geotectonic setting of some Tertiary-Quaternary Italian volcanic rocks: orogenic, anrogenic and "transitional" associations – a review. *Bull. Volcanol.* 47, 421–432.
- Di Girolamo, P., Franciosi, L., Melluso, L., Morra, V., 1996. The calc-alkaline rocks of the Campanian plain: new mineral chemical data and possible link with acidic rocks of the Pontine Island. *Period. Mineral.* 65, 305–316.
- Di Renzo, V., Di Vito, M.A., Arienzo, I., Carandente, A., Civetta, L., D'Antonio, M., Giordano, F., Orsi, G., Tonarini, S., 2007. Magmatic history of Somma-Vesuvius on the basis of new geochemical and isotopic data from deep borehole (Camaldoli della Torre). *J. Petrol.* 48, 753–784.
- Di Rocco, T., Freda, C., Gaeta, M., Mollo, S., Dallai, L., 2012. Magma chambers emplaced in carbonate substrate: petrogenesis of skarn and cumulate rocks and implications for CO₂ degassing in volcanic areas. *J. Petrol.* 53 (11), 2307–2332.
- Eiler, J.M., 2001. Oxygen isotope variations of basaltic lavas and upper mantle rocks. *Rev. Mineral. Geochem.* 43 (1), 319–364.
- Fan, W., Jiang, N., Hu, J., Liu, D., Zhao, L., Li, T., 2021. A metasomatized ^{18}O -rich veined lithospheric mantle source for ultrapotassic magmas. *Lithos* 382–383, 105964.
- Fedele, L., Scarpati, C., Lanphere, M., Melluso, L., Morra, V., Perrotta, A., Ricci, G., 2008. The Breccia Museo formation, Campi Flegrei, southern Italy: geochronology, chemostratigraphy and relationship with the Campanian ignimbrite eruption. *Bull. Volcanol.* 70, 1189–1219.
- Fedi, M., Celli, F., D'Antonio, M., Florio, G., Paoletti, V., Morra, V., 2018. Gravity modelling finds a large magma body in the deep crust below the Gulf of Naples, Italy. *Sci. Rep.* 8, 8229.
- Foley, S., Venturelli, G., Green, D.H., Toscani, L., 1987. The ultrapotassic rocks: characteristics, classification, and constraints for petrogenetic models. *Earth Sci. Rev.* 24 (2), 81–134.

- Freda, C., Gaeta, M., Misiti, V., Mollo, S., Dolfi, D., Scarlato, P., 2008. Magma-carbonate interaction: an experimental study on ultrapotassic rocks from Alban Hills (Central Italy). *Lithos* 101, 397–415.
- Fulignati, P., Panichi, C., Sbrana, A., Caliro, S., Gioncada, A., Del Moro, A., 2005. Skarn formation at the walls of the 79AD magma chamber of Vesuvius (Italy): mineralogical and isotopic constraints. *N. Jb. Min. Abh.* 181, 53–66.
- Gaeta, M., Freda, C., Christensen, J.N., Dallai, L., Marra, F., Karner, D.B., Scarlato, P., 2006. Time-dependent geochemistry of clinopyroxene from the Alban Hills (Central Italy): clues to the source and evolution of ultrapotassic magmas. *Lithos* 86 (3–4), 330–346.
- Gaeta, M., Di Rocco, T., Freda, C., 2009. Carbonate assimilation in open magmatic systems: the role of melt-bearing skarns and cumulate-forming processes. *J. Petrol.* 50 (2), 361–385.
- Gaeta, M., Freda, C., Marra, F., Arienzo, I., Gozzi, F., Jicha, B., Di Rocco, T., 2016. Paleozoic metasomatism at the origin of Mediterranean ultrapotassic magmas: constraints from time-dependent geochemistry of Colli Albani volcanic products (Central Italy). *Lithos* 244, 151–164.
- Gasperini, D., Blachert-Toft, J., Bosch, D., Del Moro, A., Macera, P., Albarède, F., 2002. Upwelling of deep mantle material through a plate window: evidence from the geochemistry of Italian basaltic volcanics. *J. Geophys. Res. Solid Earth* 107 (B12), 2367. <https://doi.org/10.1029/2001JB000418>.
- Gozzi, F., Gaeta, M., Freda, C., Mollo, S., Di Rocco, T., Marra, F., Dallai, L., Pack, A., 2014. Primary magmatic calcite reveals origin from crustal carbonate. *Lithos* 190, 191–203.
- Guarino, V., Wu, F.-Y., Lustrino, M., Melluso, L., Brotzu, P., Gomes, C.B., Ruberti, E., Tassinari, C.C.G., Svisero, D.P., 2013. U-Pb ages, Sr-Nd-isotope geochemistry and petrogenesis of kimberlites, kamacites and phlogopite-picrites of the alto Paranaiba Igneous Province, Brazil. *Chem. Geol.* 353, 65–82. <https://doi.org/10.1016/j.chemgeo.2012.06.016>.
- Guarino, V., Lustrino, M., Zanetti, A., Ruberti, E., Tassinari, C.C.G., de' Gennaro, R., Melluso, L., 2021. Mineralogy and geochemistry of a giant aegapitic magma reservoir: the Late Cretaceous Poços de Caldas potassic alkaline complex (SE Brazil). *Lithos* 398 (399), 106330. <https://doi.org/10.1016/j.lithos.2021.106330>.
- Günther, J., Prelević, D., Mertz, D., Rocholl, A., Mertz-Kraus, R., Conticelli, S., 2023. Subduction-legacy and olivine monitoring for mantle-heterogeneities of the sources of ultrapotassic magmas: the Italian case study. *Geochim. Geophys. Geosyst.* 24, e2022GC010709 <https://doi.org/10.1029/2022GC010709>.
- Iacono Marziano, G., Gaillard, F., Pichavant, M., 2007. Limestone assimilation and the origin of CO₂ emissions at the Alban Hills (Central Italy): constraints from experimental petrology. *J. Volcanol. Geotherm. Res.* 166 (2), 91–105.
- Iacono Marziano, G., Gaillard, F., Pichavant, M., 2008. Limestone assimilation by basaltic magmas: an experimental re-assessment and application to Italian volcanoes. *Contrib. Mineral. Petro.* 155, 719–738.
- Iovine, R.S., Mazzeo, F.C., Wörner, G., Pelullo, C., Cirillo, G., Arienzo, I., Pack, A., D'Antonio, M., 2018. Coupled δ¹⁸O-δ¹⁷O and ⁸⁷Sr/⁸⁶Sr isotope compositions suggest a radiogenic and ¹⁸O-enriched magma source for Neapolitan volcanoes. *Lithos* 316–317, 199–211.
- Jolis, E.M., Freda, C., Troll, V.R., Deegan, F.M., Blythe, L.S., McLeod, C.L., Davidson, J.P., 2013. Experimental simulation of magma–carbonate interaction beneath Mt. Vesuvius, Italy. *Contrib. Mineral. Petro.* 166, 1335–1353.
- Jolis, E.M., Troll, V.R., Harris, C., Freda, C., Gaeta, M., Orsi, G., Siebe, C., 2015. Skarn xenolith record crustal CO₂ liberation during Pompeii and Pollena eruptions, Vesuvius volcanic system, central Italy. *Chem. Geol.* 415, 17–36.
- Joron, J.L., Metrich, N., Rosi, M., Santacroce, R., Sbrana, A., 1987. Chemistry and petrography. In: Santacroce, R. (Ed.), Somma Vesuvius, C.N.R. Quaderni di “La Ricerca Scientifica”, 8, pp. 105–174.
- Klaiver, M., Djuly, T., de Graaf, S., Sakes, A., Wijibrans, J.R., Davies, G., Vroon, P.Z., 2015. Temporal and spatial variations in provenance of eastern Mediterranean Sea sediments: implications for Aegean and Aeolian arc volcanism. *Geochim. Cosmochim. Acta* 153, 149–168.
- Landi, P., Bertagnini, A., Rosi, M., 1999. Chemical zoning and crystallization mechanism in the magma chamber of the Pomici di base plinian eruption of Somma-Vesuvius (Italy). *Contrib. Mineral. Petro.* 135, 179–197.
- Laurenzi, M.A., Braschi, E., Casalini, M., Conticelli, S., 2015. New 40Ar-39Ar dating and revision of the geochronology of the Monte Amiata volcano, Central Italy. *Ital. J. Geosci.* 134, 255–265. <https://doi.org/10.3301/IJG.2015.11>.
- Le Bas, M.J., Le Maître, R.W., Streckeisen, A., Zanettin, B., 1986. A chemical classification of volcanic rocks based on the total alkali-silica diagram. *J. Petrol.* 27, 745–750. <https://doi.org/10.1093/petrology/27.3.745>.
- Lustrino, M., Cuccinello, C., Melluso, L., Tassinari, C.C.G., de' Gennaro, R., Serracino, M., 2012. Petrogenesis of Cenozoic volcanic rocks in the NW sector of the Gharyan volcanic field, Libya. *Lithos* 155, 218–235. <https://doi.org/10.1016/j.lithos.2012.09.003>.
- Lyubetskaya, T., Korenaga, J., 2007. Chemical composition of Earth's primitive mantle and its variance: 1. Methods and results. *J. Geophys. Res.* 112, B03211. <https://doi.org/10.1019/2005JB004223>.
- Marianelli, P., Métrich, N., Sbrana, A., 1999. Shallow and deep reservoirs involved in magma supply of the 1944 eruption of Vesuvius. *Bull. Volcanol.* 61, 48–63.
- Mattey, D., Lowry, D., Macpherson, C., 1994. Oxygen isotope composition of mantle peridotite. *Earth Planet. Sci. Lett.* 128, 231–241.
- Matthews, A., Stolper, E.M., Eiler, J.M., Valley, J.W., 1998. Oxygen isotope fractionation among melts, minerals and rocks. *Mineral. Mag.* 62A, 971–972.
- Mazzeo, F.C., D'Antonio, M., Arienzo, I., Aulinás, M., Di Renzo, V., Gimeno, D., 2014. Subduction-related enrichment of the Neapolitan volcanoes (southern Italy) mantle source: new constraints on the characteristics of the slab-derived components. *Chem. Geol.* 386, 165–183.
- Mazzeo, F.C., Arienzo, I., Aulinás, M., Casalini, M., Di Renzo, V., D'Antonio, M., 2018. Mineralogical, geochemical and isotopic characteristics of alkaline mafic igneous rocks from Punta delle Pietre Nere (Gargano, southern Italy). *Lithos* 308–309, 316–328.
- Melluso, L., Conticelli, S., D'Antonio, M., Mirco, N.P., Saccani, E., 2003. Petrology and mineralogy of wollastonite- and melilite-bearing paralavas from the central Apennines, Italy. *Am. Mineral.* 88 (8–9), 1287–1299.
- Melluso, L., de' Gennaro, R., Fedele, L., Franciosi, L., Morra, V., 2012. Evidence of crystallization in residual, Cl-F-rich, aegapitic, trachyphonolitic magmas and primitive Mg-rich basalt-trachyphonolite interaction in the lava domes of the Phleorean Fields (Italy). *Geol. Mag.* 149 (3), 532–550. <https://doi.org/10.1017/S0016756811000902>.
- Melluso, L., Morra, V., Guarino, V., de' Gennaro, R., Franciosi, L., Grifa, C., 2014. The crystallization of shoshonitic to peralkaline trachyphonolitic magmas in a H₂O-Cl-F-rich environment at Ischia (Italy), with implications for the feeder system of the Campania Plain volcanoes. *Lithos* 210–211, 242–259. <https://doi.org/10.1016/j.lithos.2014.10.002>.
- Melluso, L., Cuccinello, C., le Roex, A.P., Morra, V., 2016. The geochemistry of primitive volcanic rocks of the Ankaratra volcanic complex, and source enrichment processes in the genesis of the Cenozoic magmatism in Madagascar. *Geochim. Cosmochim. Acta* 185, 435–452. <https://doi.org/10.1016/j.gca.2016.04.005>.
- Melluso, L., Scarpatti, C., Zanetti, A., Sparice, D., de' Gennaro, R., 2022. The petrology and geochemistry of zoned, phonolitic Plinian and sub-Plinian eruptions of Somma-Vesuvius, Italy: role of accessory phase removal, independently filled magma reservoirs with time, and transition from slightly to highly silica undersaturated series in an ultrapotassic stratovolcano. *Lithos* 430–431, 106854. <https://doi.org/10.1016/j.lithos.2022.106854>.
- Middlemost, E.A.K., 1975. The basalt clan. *Earth-Sci. Rev.* 11, 337–364.
- Minissale, S., Casalini, M., Cuccinello, C., Balagizi, C., Tedesco, D., Boudoire, G., Morra, V., Melluso, L., 2022. The geochemistry of recent Nyamulagira and Nyiragongo potassic lavas, Virunga Volcanic Province, and implications on the enrichment processes in the mantle lithosphere of the Tanzania-Congo craton. *Lithos* 420–421, 106696. <https://doi.org/10.1016/j.lithos.2022.106696>.
- Mollo, S., Del Gaudio, P., Ventura, G., Iezzi, G., Scarlato, P., 2010. Dependence of clinopyroxene composition on cooling rate in basaltic magmas: implications for thermobarometry. *Lithos* 118 (3–4), 302–312.
- Pappalardo, L., Piochi, M., D'Antonio, M., Civetta, L., Petrini, R., 2002. Evidence for multi-stage magmatic evolution during the past 60 kyr at Campi Flegrei (Italy) deduced from Sr, Nd and Pb isotope data. *J. Petrol.* 43 (8), 1415–1434.
- Peccerillo, A., 1998. Relationships between ultrapotassic and carbonate-rich volcanic rocks in Central Italy: petrogenetic and geodynamic implications. *Lithos* 43, 267–279.
- Peccerillo, A., 2001. Geochemical similarities between the Vesuvio, Phleorean fields and Stromboli volcanoes: petrogenetic, geodynamic and volcanological implications. *Mineral. Petrol.* 73, 93–105.
- Peccerillo, A., 2005. Plio-Quaternary Volcanism in Italy: Petrology, Geochemistry, Geodynamics. Springer-Verlag, Berlin. 365 pp.
- Peccerillo, A., 2017. The Roman Province. In: Cenozoic Volcanism in the Tyrrhenian Sea Region. Advances in Volcanology. Springer, Cham. https://doi.org/10.1007/978-3-319-42491-0_4.
- Piana Agostinetti, N., Chiarabba, C., 2008. Seismic structure beneath Mt Vesuvius from receiver function analysis and local earthquakes tomography: evidences for location and geometry of the magma chamber. *Geophys. J. Int.* 175 (3), 1298–1308.
- Pichavant, M., Scaillet, B., Pommier, A., Iacono-Marziano, G., Cioni, R., 2014. Nature and evolution of primitive Vesuvius magmas: an experimental study. *J. Petrol.* 55, 2281–2310.
- Piochi, M., Ayuso, R.A., De Vivo, B., Somma, R., 2006. Crustal contamination and crystal entrapment during polybaric magma evolution at Mt. Somma-Vesuvius volcano, Italy: geochemical and Sr isotope evidence. *Lithos* 86, 303–329.
- Plank, T., Langmuir, C.H., 1998. The chemical composition of subducting sediments and its consequence for the crust and mantle. *Chem. Geol.* 145, 325–394.
- Ren, H., Casalini, M., Conticelli, S., Chen, C., Foley, S.F., Feng, L., Liu, Y., 2024. Calcium isotope compositions of subduction-related leucite-bearing rocks: implications for the calcium isotope heterogeneity of the mantle and carbonate recycling in convergent margins. *Geochim. Cosmochim. Acta* 364, 100–113. <https://doi.org/10.1016/j.gca.2023.11.022>.
- Rittmann, A., 1933. Die geologische bedingte evolution und differentiation des Somma-Vesuvius magnas. *Zeit. Vulkan.* 15, 1–2.
- Rogers, N.W., Hawkesworth, C.J., Parker, R.J., Marsh, J.S., 1985. The geochemistry of potassic lavas from Vulcini, Central Italy, and implications for mantle enrichment processes beneath the Roman region. *Contrib. Mineral. Petro.* 90, 244–257.
- Rosatelli, G., Castorina, F., Consalvo, A., Brozzetti, F., Ciavardelli, D., Perna, M.G., Bell, K., Bello, S., Stoppa, F., 2023. Elemental abundances and isotopic composition of Italian limestones: glimpses into the evolution of the Tethys. *J. Asian Earth Sci.* X 9, 100136.
- Rouchon, V., Gillot, P.Y., Quidelleur, X., Chiesa, S., Floris, B., 2008. Temporal evolution of the Roccamonfina volcanic complex (Pleistocene), Central Italy. *J. Volcanol. Geotherm. Res.* 177, 500–514.
- Santacroce, R., 1987. Somma-Vesuvius. In: C.N.R. Quaderni di “La Ricerca Scientifica”, 114, 251 pp.
- Santacroce, R., Cioni, R., Marianelli, P., Sbrana, A., Sulpizio, R., Zanchetta, G., Donahue, D.J., Joron, J.L., 2008. Age and whole rock-glass compositions of proximal pyroclastics from the major explosive eruptions of Somma-Vesuvius: A review as a tool for distal tephrostratigraphy. *J. Volcanol. Geotherm. Res.* 177 (1), 1–18. <https://doi.org/10.1016/j.jvolgeores.2008.06.009>.

- Savelli, C., 1967. The problem of rock assimilation by Somma-Vesuvius magma - I. Composition of Somma and Vesuvius lavas. *Contrib. Mineral. Petrol.* 16, 328–353.
- Savelli, C., 1968. The problem of rock assimilation by Somma-Vesuvius magma - II. Composition of sedimentary rocks and carbonate ejecta from the Vesuvius area. *Contrib. Mineral. Petrol.* 18, 43–64.
- Skora, S., Blundy, J.D., Brooker, R.A., Green, E.C.R., de Hoog, J.C.M., Connolly, J.A.D., 2015. Hydrous phase relations and trace element partitioning behaviour in calcareous sediments at subduction-zone conditions. *J. Petrol.* 56, 953–980.
- Sparice, D., Scarpati, C., Mazzeo, F.C., Petrosino, P., Arienzo, I., Gisbert, G., Petrelli, M., 2017. New proximal tephras at Somma-Vesuvius: evidences of a pre-caldera, large (?) explosive eruption. *J. Volcanol. Geotherm. Res.* 335, 71–81.
- Stoppa, F., Rukhlov, A.S., Bell, K., Schiazza, M., Vichi, G., 2014. Lamprophyres of Italy: Early Cretaceous alkaline lamprophyres of southern Tuscany, Italy. *Lithos* 188, 97–112.
- Stormer, J.C., Nicholls, J., 1978. XLFrac: a program for interactive testing of magmatic differentiation models. *Comput. Geosci.* 4, 143–159.
- Taylor, H.P., Sheppard, S.M.F., 1986. Igneous rocks: I. Process of isotopic fractionation and isotope systematics. In: *Reviews in Mineralogy*, vol. 16. Mineral. Soc. Am., Book Crafters, Inc., Chelsea, Michigan, pp. 227–271.
- van Bergen, M.J., Ghezzo, C., Ricci, C.A., 1983. Minette inclusions in the rhyodacitic lavas of Mt. Amiata (Central Italy): mineralogical and chemical evidence of mixing between Tuscan and Roman type magmas. *J. Volcanol. Geotherm. Res.* 19, 1–35.
- Washington, H.S., 1906. The Roman Comagmatic region. In: *Carnegie Institution of Washington Yearbook*, 36, pp. 1–220.
- Wöelki, D., Haase, K.M., Schoenhofen, M.V., Beier, C., Regelous, M., Krumm, S.H., Günther, T., 2018. Evidence for melting of subducting carbonate-rich sediments in the western Aegean Arc. *Chem. Geol.* 483, 463–473.
- Zhang, K.-J., Li, Q.-H., Yan, L.-L., Zeng, L., Lu, L., Zhang, Y.-X., Hui, J., Jin, X., Tang, X.-C., 2017. Geochemistry of limestones deposited in various plate tectonic settings. *Earth Sci. Rev.* 167, 27–46.
- Zhao, Z.-F., Zheng, Y.-F., 2003. Calculation of oxygen isotope fractionation in magmatic rocks. *Chem. Geol.* 193, 59–80.
- Zollo, A., Gasparini, P., Virieux, J., Le Meur, H., De Natale, G., Biella, G., Boschi, E., Capuano, P., de Franco, R., dell'Aversana, P., de Matteis, R., Iannaccone, G., Mirabile, L., Vilardo, G., 1996. Seismic evidence for a low-velocity zone in the upper crust beneath Mount Vesuvius. *Science* 274 (5287), 592–594.